

Supplementary Information

Alkaline earth-organic frameworks with amino derivatives of 2,6-naphthalene dicarboxylates: structural studies and fluorescence properties

Stavros A. Diamantis,[†] Antonios Hatzidimitriou,[†] Alexios K. Plessas,^{||} Anastasia Pournara,[‡] Manolis J. Manos,[‡] Giannis S. Papaefstathiou,^{||,*} and Theodore Lazarides^{†,*}

[†] Laboratory of Inorganic Chemistry, Department of Chemistry, Aristotle University of Thessaloniki, Thessaloniki, 54124, Greece

^{||} Laboratory of Inorganic Chemistry, Department of Chemistry, National and Kapodistrian University of Athens, Panepistimiopolis, Zografou 15771, Greece.

[‡] Laboratory of Inorganic Chemistry, Department of Chemistry, University of Ioannina, Ioannina 45110, Greece

Table of Contents

Synthesis of H ₂ ANDC and H ₂ NDC-(NO ₂) ₂	S4
Figure S1. ¹ H NMR spectra of H ₂ NDC-(NO ₂) ₂	S4
Figure S2. ¹³ C NMR spectra of H ₂ NDC-(NO ₂) ₂	S5
H ₂ DANDC synthesis	S5
Figure S3. ¹ H NMR spectra of H ₂ DANDC	S6
Figure S4. ¹³ C NMR spectra of H ₂ DANDC	S6
Figure S5. Mass spectra (ESI-MS) of H ₂ DANDC ligand	S7
Synthesis of AEMOFs	S7
Figure S6. PXRD of 1	S11
Figure S7. PXRD of 2	S11
Figure S8. PXRD of 3	S12
Figure S9. PXRD of 4	S12
Figure S10. PXRD of 5	S13
Figure S11. PXRD of 6	S13
Figure S12. PXRD of 7	S14
Figure S13. PXRD of 8	S14
Crystal data and structure refinement for the MOFs.	S14
Table S1. Selected crystal data for 1 - 4	S15
Table S2. Selected crystal data for 5 - 8	S16
Figure S14. Representation of the SBU and) 3-D of 7	S17
Figure S15. The deconstruction of the frameworks 1,5,7 and 8	S17
Figure S16. The deconstruction of the framework 6	S18
Figure S16. The deconstruction of the framework 2	S19
Figure S17. The deconstruction of the framework 3	S20
Figure S18. The deconstruction of the framework 4	S21
Table S3-S10. Selected bond lengths and angles for compounds 1-8	S22
Figure S19. The TGA and DTG curves for 1	S35
Figure S20. The TGA and DTG curves for 2	S36
Figure S21. The TGA and DTG curves for 3	S37
Figure S22. The TGA and DTG curves for 4	S38
Figure S23. The TGA and DTG curves for 5	S39
Figure S24. The TGA and DTG curves for 6	S40

Figure S25. The TGA and DTG curves for 7	S41
Figure S26. The TGA and DTG curves for 8	S42
Figure S27. Emission spectra of the ligands in MeOH.....	S43
Figure S28. Excitation spectra of the ligands in MeOH.....	S43
Figure S29. UV-Vis spectra of the ligands in MeOH.....	S44
Figure S30. UV-Vis spectra of the H ₂ ANDC ligand in MeOH/DMF mixtures.....	S44
Figure S31. UV-Vis spectra of the H ₂ DANDC ligand in MeOH/DMF mixtures.....	S45
Figure S32. UV-Vis spectra of the H ₂ ANDC ligand in MeOH/DMF mixtures.....	S45
Figure S33. UV-Vis spectra of the H ₂ DANDC ligand in MeOH/DMF mixtures.....	S46
Figure S34. Solid state excitation spectra of 1-3	S46
Figure S35. Solid state excitation spectra of 4-8	S47
References.	S47

Materials and methods. The analytical instruments used in this work are the same as those reported previously.¹ All chemicals were used as received from the usual commercial sources (Sigma Aldrich, Alfa Aesar and TCI).

Ligand synthesis

H₂ANDC was synthesized as previously reported.²

H₂DANDC

Synthesis of 4,8-dinitronaphthalene-2,6-dicarboxylic acid H₂NDC-(NO₂)₂. 2,6-Naphthalene dicarboxylic acid (1.00 g, 4.63 mmol) was dissolved in concentrated H₂SO₄ (80 ml) and then nitric acid (825 μ L, 3 eq) was added dropwise under vigorous stirring. The mixture was stirred at room temperature for 2 hours and then poured onto ice (400 ml) to form a yellow solid which was isolated by vacuum filtration and washing with cold water (3 x 100 mL). The resulting solid was recrystallized from acetic acid and washed with water (5 x 20 mL) to afford the pure product. Yield: 1.3 gr (4.24 mmoles, 92%). ¹H NMR (500 MHz, DMSO): δ (ppm) = 11.95 (br, 2 H), 9.26 (s, 2 H), 8.80 (s, 2 H), ¹³C NMR (126 MHz, DMSO): δ (ppm) = 165.32, 148.10, 132.20, 130.56, 126.74, 125.22.

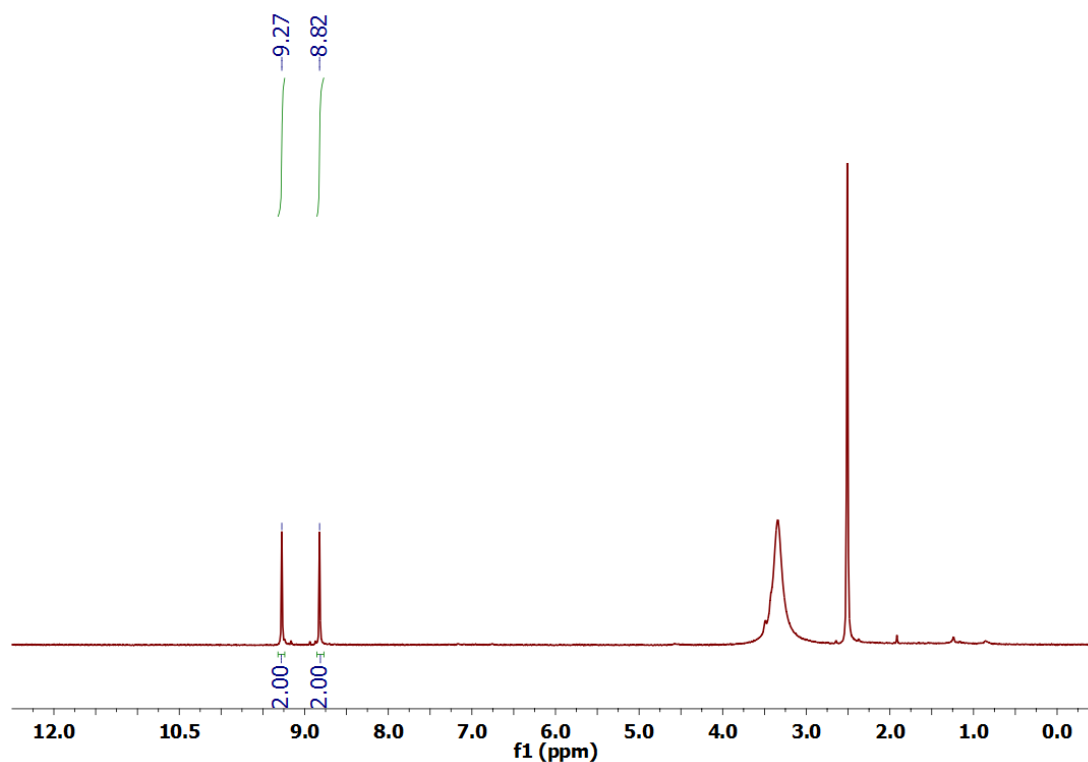


Figure S1. ^1H NMR spectra of $\text{H}_2\text{NDC}-(\text{NO}_2)_2$ (DMSO- d_6 , 500 MHz)

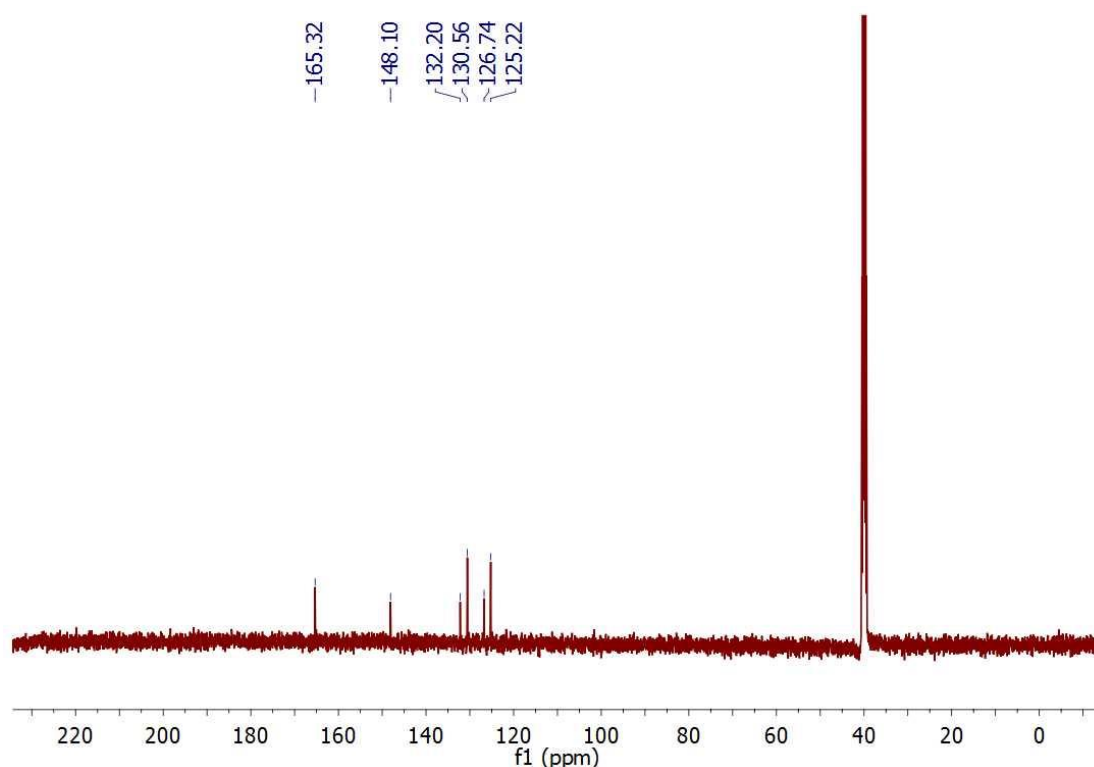


Figure S2. ^{13}C NMR spectra of $\text{H}_2\text{NDC}-(\text{NO}_2)_2$ (DMSO- d_6 , 126 MHz)

Synthesis of 4,8-diaminonaphthalene-2,6-dicarboxylic acid H_2DANDC . 4,8-dinitronaphthalene-2,6-dicarboxylic acid (1.3 gr, 4.24 mmol) was dissolved in 300 ml MeOH and the solution was stirred under $\text{Ar}(\text{g})$ for 10 minutes. To this solution, 100 mg of 10% Pd / C was added under $\text{Ar}(\text{g})$ and the mixture was stirred for additional 10 minutes, followed by vigorous stirring under H_2 atmosphere for 24 hours at room temperature. The solvent was concentrated under vacuum and aqueous NaOH (1 M) was added aqueous solution of NaOH (1M). The reaction mixture was then filtrated through Celite and acidified with acetic acid to afford a deep green precipitate. The solid was filtered, washed with water and dried under vacuum for 12 h. Yield 930 mg (3.77 mmol, 89%). ^1H NMR (500 MHz, DMSO- d_6): δ (ppm) = 7.90 (s, 2 H), 7.16 (s, 2 H), 5.82 (br, 4 H). ^{13}C NMR (126 MHz, DMSO- d_6): δ (ppm) 168.67, 146.75, 128.85, 125.28, 112.77, 107.64. MS (ESI $^+$) m/z: calc: 244.2; found: 288 $[\text{M}+\text{H}+\text{MeCN}]^+$. IR (KBr pellets, cm^{-1}): 3437 m, 3348 m, 3237 w, 3082 w, 2968 w, 1670 m, 1632 m, 1584 m, 1541 s, 1534 s, 1508 s, 1442 s, 1421 m, 1370 m, 1353 w, 1308 s, 1264 m, 1239 w, 903 m.

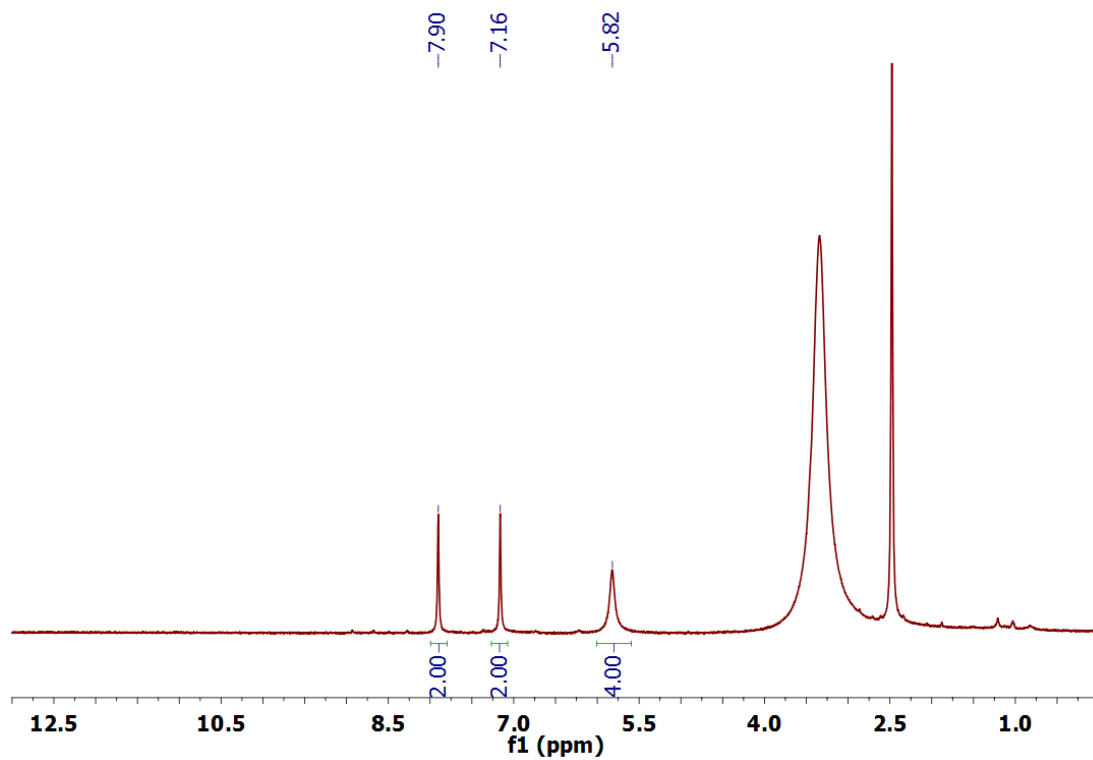


Figure S3. ^1H NMR spectra of $\text{H}_2\text{NDC}-(\text{NH}_2)_2$ (DMSO- d_6 , 500 MHz)

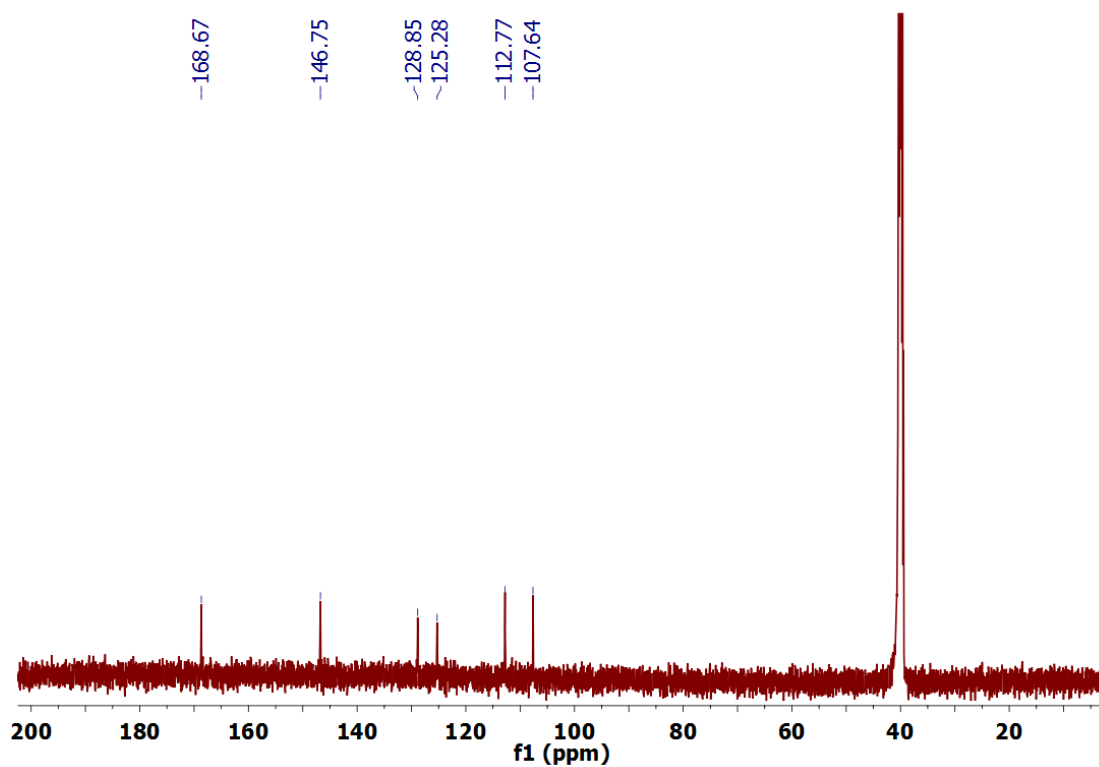


Figure S4. ^{13}C NMR spectra of $\text{H}_2\text{NDC}-(\text{NH}_2)_2$ (DMSO- d_6 , 126 MHz)

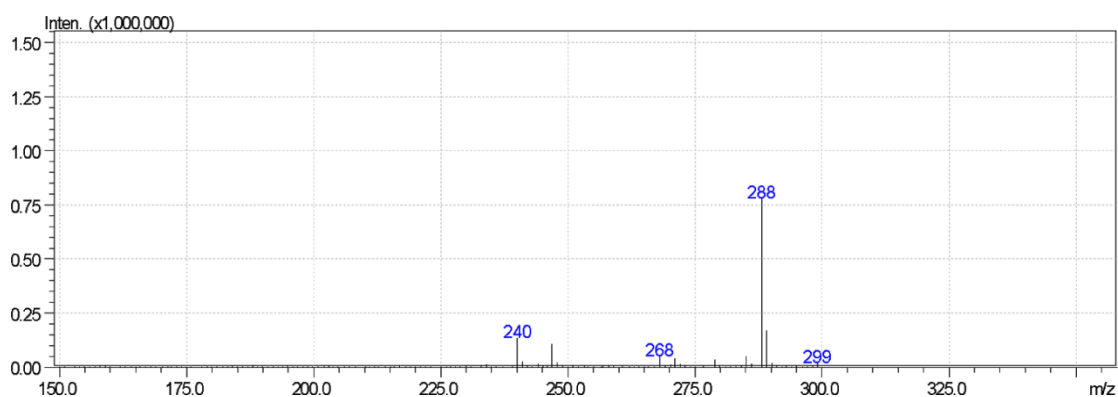


Figure S5. Mass spectra (ESI-MS) of H₂NDC-(NH₂)₂ ligand, [M]⁺+H+ACN.

Synthesis of the MOFs

[Ca₄(μ₄-H₂O)(ANDC)₄(DMF)₄]·6 DMF (1)

Ca(NO₃)₂·4H₂O (15.3 mg, 0.065 mmol) or CaCl₂·2H₂O (9.6 mg, 0.065 mmol) was added as a solid into a solution of H₂ANDC (15.0 mg, 0.065 mmol) in 3 mL DMF/H₂O (9:1 v/v), in a 23 mL glass vial. The mixture was sonicated at room temperature for *ca.* 3 min and then placed in an oven at 110°, remained undisturbed at this temperature for 24 h and was then cooled slowly to room temperature. Cubic brown crystals of **1** were isolated by filtration, washed with DMF and dried under vacuum for 20 hours. Yield 17.0 mg (~63%). IR (KBr pellets, cm⁻¹): 3393 br, 2924 w, 2848 w, 1655 w, 1625 w, 1600 m, 1552 s, 1497 m, 1426 s, 1367 s, 1141 w, 1101 w, 802 m, 798 m

Sr₂(ANDC)₂(DMF)₂(H₂O)]·DMF (2)

Sr(NO₃)₂ (15.0 mg, 0.065 mmol) or SrCl₂·6H₂O (17.3 mg, 0.065 mmol) was added as solid into a solution of H₂ANDC (15.0 mg, 0.065 mmol) in 3 ml DMF/H₂O (9:1 v/v), in a 23 mL glass vial. The mixture was sonicated at room temperature for *ca.* 3 min and then placed in an oven at 120°, remained undisturbed at this temperature for 24 h and was then cooled slowly to room temperature.. Needle-like brown crystals of **MOF-2** were isolated by filtration, washed with DMF and dried under vacuum for 20 hours. Yield: 17.0 mg (~61%). IR (KBr pellets, cm⁻¹): 3424 br, 3240 m, 2926 w, 1660 m, 1660 s, 1558 s, 1498 s, 1425 s, 1367 s, 1140 w, 1101 w, 802 m, 797 m.

Ba₂(ANDC)₄(μ₂-DMF)₂(DMF)₂ (3)

Ba(NO₃)₂ (17.0 mg, 0.065 mmol) or BaCl₂·2H₂O (15.9 mg, 0.065 mmol) was added as solid into a solution of H₂ANDC (15.0 mg, 0.065 mmol) in 3 ml DMF/H₂O (9:1 v/v), in a 23 mL glass vial. The procedure followed was identical to that for the synthesis of **2**. Needle-like brown crystals of **3** were isolated by filtration, washed with DMF and dried under vacuum for 20 hours. Yield: 18.0 mg (~60%). IR (KBr pellets, cm⁻¹): 3420 br, 3340 m, 2955 w, 2924 m, 1646 m, 1597 m, 1553 s, 1497 m, 1418 m, 1363 s, 1135 w, 1093 w, 795 m, 786 m.

Mg₈(DANDC)₈(H₂O)₅(DMF)₃·5 DMF (4)

Mg(OAc)₂·4H₂O (13.2 mg, 0.061 mmol) was added as solid into a solution of H₂DANDC (15.0 mg, 0.061 mmol) in a Teflon cup. The mixture was sonicated at room temperature for *ca.* 3 min and then, the Teflon cup was transferred into a 23 mL stainless steel autoclave. The autoclave was sealed and placed in an oven at 120 °C, remained undisturbed at this temperature for 24 h and was then cooled to room temperature. Needle-like brown crystals of **4** were isolated by filtration, washed with DMF and dried under vacuum for 20 hours. Yield 16.5 (~76%). IR (KBr pellets, cm⁻¹): 3373 m, 3323 m, 3217 m, 3082 w, 2927 w, 1664 s, 1602 s, 1577 m, 1508 s, 1437 s, 1366 s, 1280 w, 1110 m, 794 m.

Ca₄(μ₄-H₂O)(DANDC)₄(H₂O)₃(DMF)₃·(2 H₂O)(4 DMF) (5)

CaCl₂·2H₂O (9.0 mg, 0.061 mmol) or Ca(NO₃)₂·4H₂O (14.4 mg, 0.061 mmol) was added as solid into a solution of H₂DANDC (15.0 mg, 0.061 mmol) in 3 ml DMF/H₂O (9:1 v/v), in a 23 mL glass vial. The procedure followed was identical to that for the synthesis of **2**. Prism-like brown crystals of **5** were isolated by filtration, washed with DMF and dried under vacuum for 20 hours. Yield: 18.0 mg (~73%). IR (KBr pellets, cm⁻¹): 3430 m, 3345 m, 3243 m, 3082 w, 2927 w, 1935 w, 1664 s, 1652 s, 1595 m, 1560 m, 1508 s, 1444 s, 1382 s, 1375 s, 1103 w, 798 m

Sr₂₄(μ₄-H₂O)₆(NDC-(NH₂)₂)₂₄(DMF)₂₄(H₂O)(56 DMF) (6)

Sr(NO₃)₂ (13.0 mg, 0.061 mmol) was added as solid into a solution of H₂DANDC (15.0 mg, 0.061 mmol) in 3 ml DMF/H₂O (9:1 v/v), in a 23 mL glass vial. The procedure

followed was identical to that for the synthesis of **2**. Prism-like brown crystals of **6** were isolated by filtration, washed with DMF and dried under vacuum for 20 hours. Yield: 18.8 mg (~53%). IR (KBr pellets, cm^{-1}): 3421 br, 2961 w, 2925 m, 2860 w, 1656 m, 1590 m, 1560 m, 1534 m, 1508 s, 1437 s, 1383 s, 1281 m, 793 m.

[(Sr₈(μ -Cl)₂(DANDC)₈(DMF)₈(Sr(DMF)₄)₃)]Cl₄(7 DMF) (7**)**

SrCl₂·6H₂O (16.3 mg, 0.061 mmol) was added as solid into a solution of H₂DANDC (15.0 mg, 0.061 mmol) in 3 ml DMF/H₂O (9:1 v/v), in a 23 mL glass vial. The procedure followed was identical to that for the synthesis of **2**. Prism-like brown crystals of **6** were isolated by filtration, washed with DMF and dried under vacuum for 20 hours. Yield: 17.5 mg (~64%). IR (KBr pellets, cm^{-1}): 3437 m, 3348 m, 3234 m, 2961 w, 2936 m, 1662 s, 1592 m, 1560 m, 1503 s, 1438 s, 1371 s, 1283 w, 1244 w, 1104 m, 793 m.

[Ba₅(μ -Cl)(DANDC)₄(H₂O)₆]]Cl·(2 H₂O)(7 DMF) (8**)**

BaCl₂·2H₂O (14.7 mg, 0.061 mmol) was added as solid into a solution of H₂DANDC (15.0 mg, 0.061 mmol) in 3 ml DMF/H₂O (9:1 v/v), in a 23 mL glass vial. The procedure followed was identical to that for the synthesis of **2**. Prism-like brown crystals of **6** were isolated by filtration, washed with DMF and dried under vacuum for 20 hours. Yield: 17.8 mg (~62%). IR (KBr pellets, cm^{-1}): 3411 m, 3327 m, 3227 w, 2927 w, 1655 s, 1584 s, 1553 s, 1502 s, 1434 s, 1365 s, 1287 w, 1258 w, 1106 w, 793 m, 780 m.

Single crystals of the MOFs were obtained from reaction mixtures according to the described synthetic procedures. For the structural determination of compounds **1-8**, single crystals of the respective MOF were mounted on a Bruker Kappa APEX II diffractometer, equipped with a triumph monochromator at ambient temperature. Diffraction measurements were recorded using MoK α radiation. The data were collected at 120-130 K over a full sphere of reciprocal space. Intensity data were collected using ω and χ scan mode. The frames collected for each crystal were integrated with the Bruker SAINT software package³ using a narrow-frame algorithm. Data were corrected for absorption using the numerical method (SADABS)⁴ based on crystal dimensions.

The powder X-ray diffraction (PXRD) data of compounds 1-8 are in agreement with the simulated PXRD patterns of the compounds (Fig. S5-12 respectively) thereby confirming that the analyzed single crystals are representative of the bulk samples. All structures were solved using the SUPERFLIP⁵ package and were refined by the full-matrix least-squares method on F² using the CRYSTALS package version 14.40b.⁶ All non-hydrogen atoms have been refined anisotropically except in the case of disordered atoms. All hydrogen atoms were found at their expected positions and refined using soft constraints. By the end of the refinement, they were positioned using riding constraints. CCDC 2033666-2033673 contain the supplementary crystallographic data for this paper. These data can be obtained free of charge via www.ccdc.cam.ac.uk/data_request/cif. The crystal data, details of data collection and structure refinement for MOFs **1 -8** are given in Tables S1 and S2. Illustrations were drawn by the Mercury program.⁷ Further details on the crystallographic studies as well as atomic displacement parameters are given in the cif files.

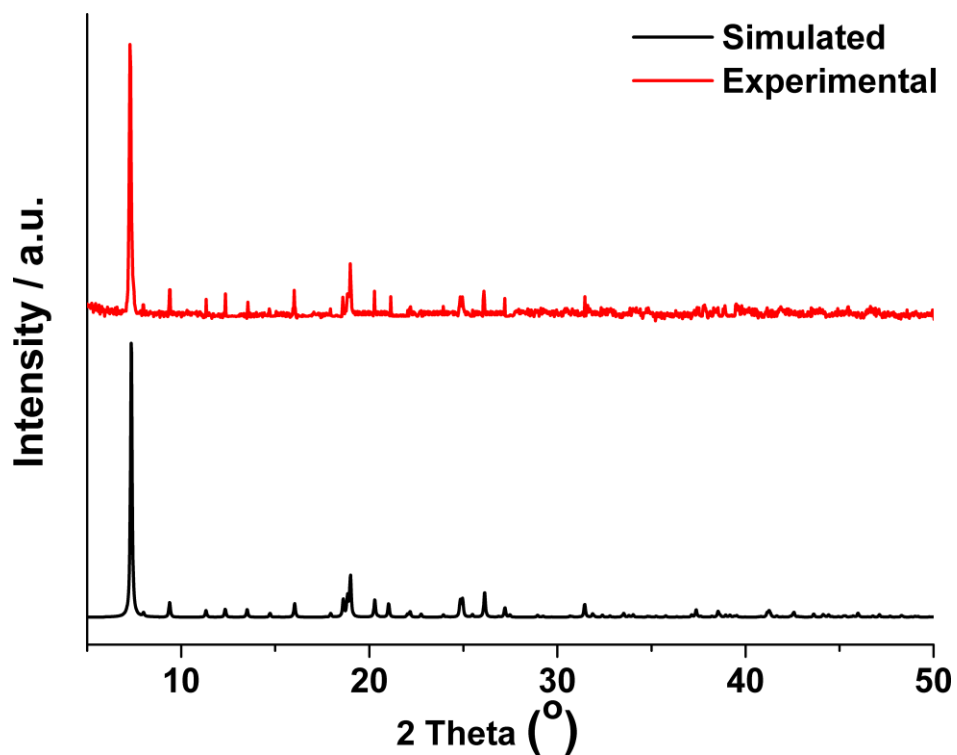


Figure S6. Simulated and experimental PXRD pattern of **1** (black and red respectively).

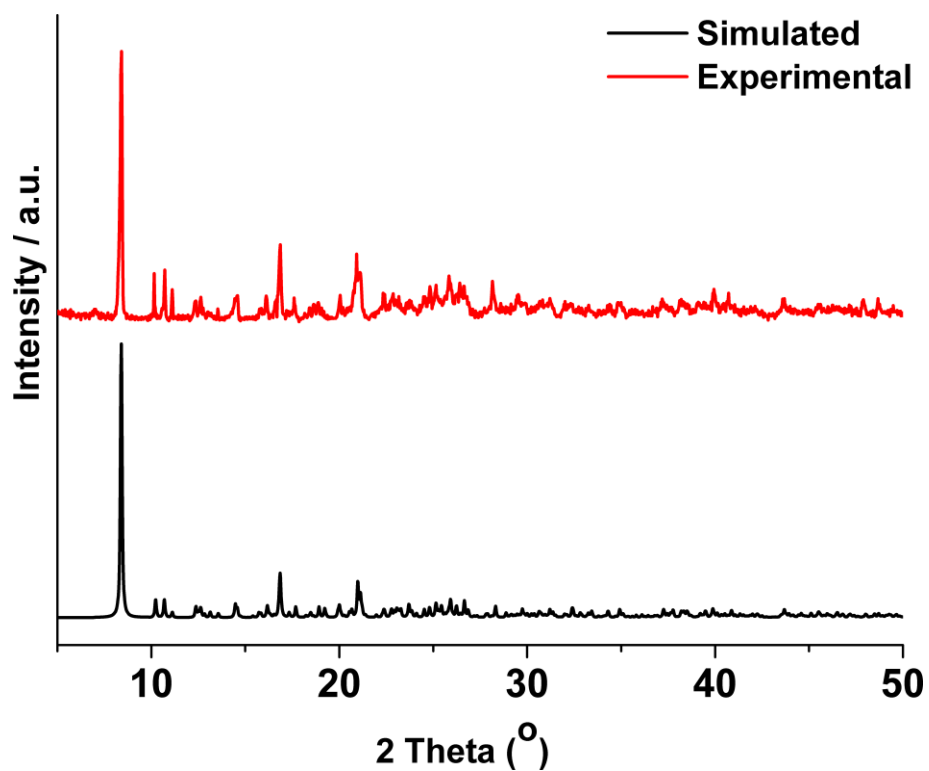


Figure S7. Simulated and experimental PXRD pattern of **2** (black and red respectively).

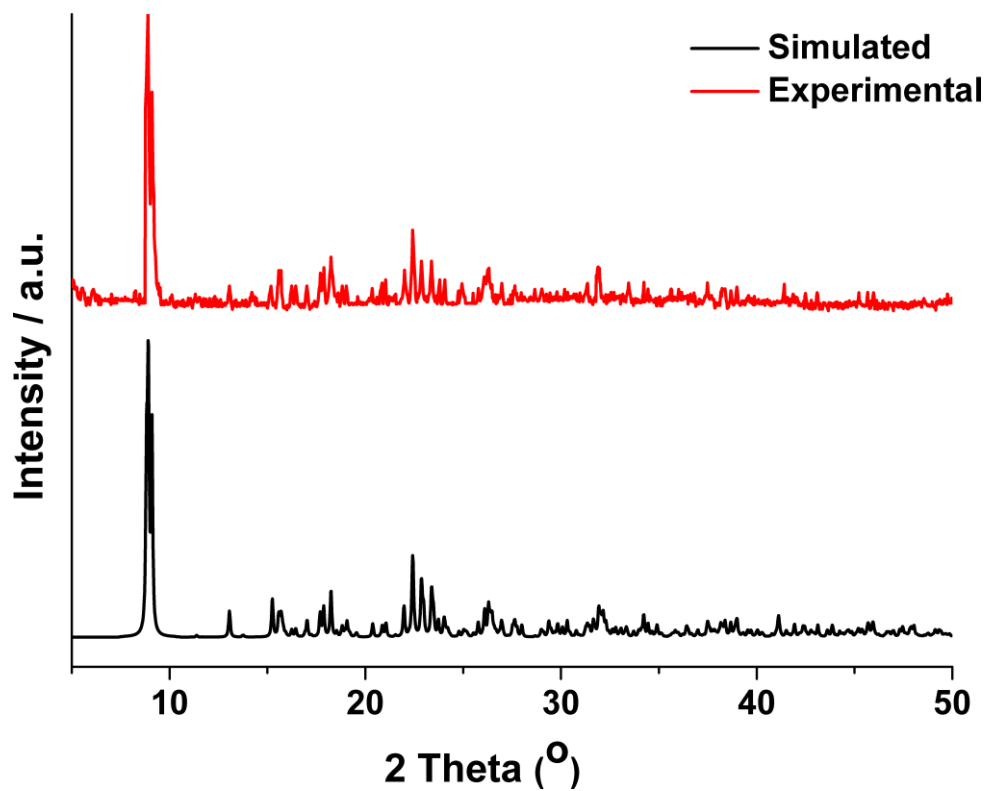


Figure S8. Simulated and experimental PXRD pattern of **3** (black and red respectively).

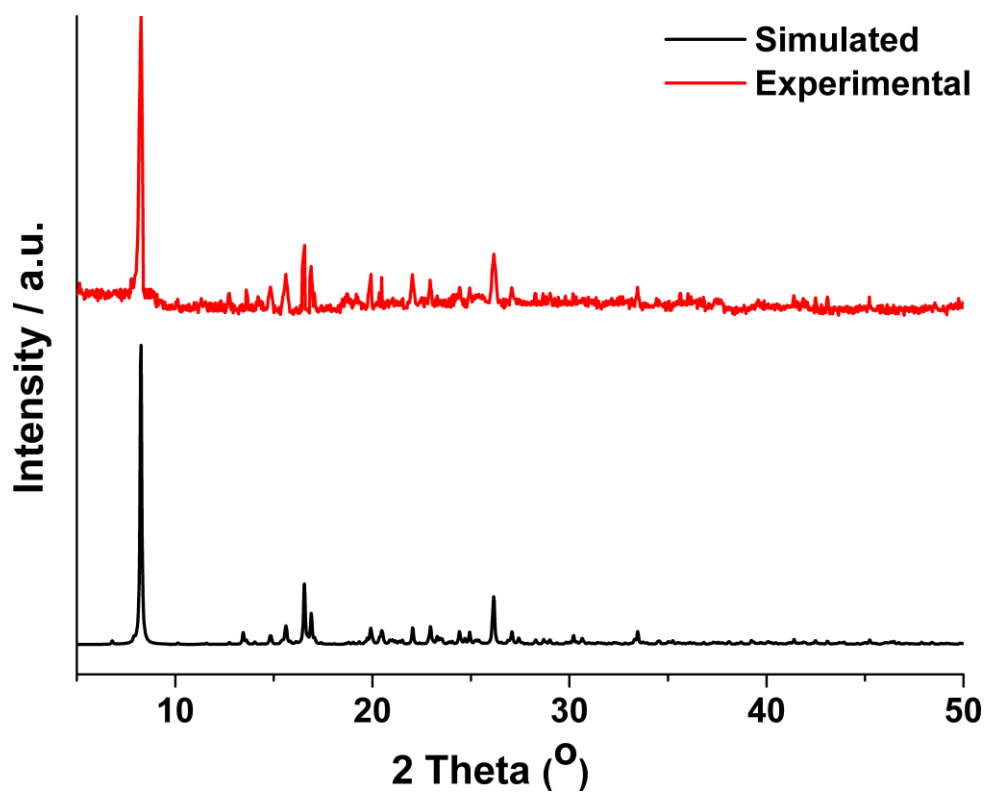


Figure S9. Simulated and experimental PXRD pattern of **4** (black and red respectively).

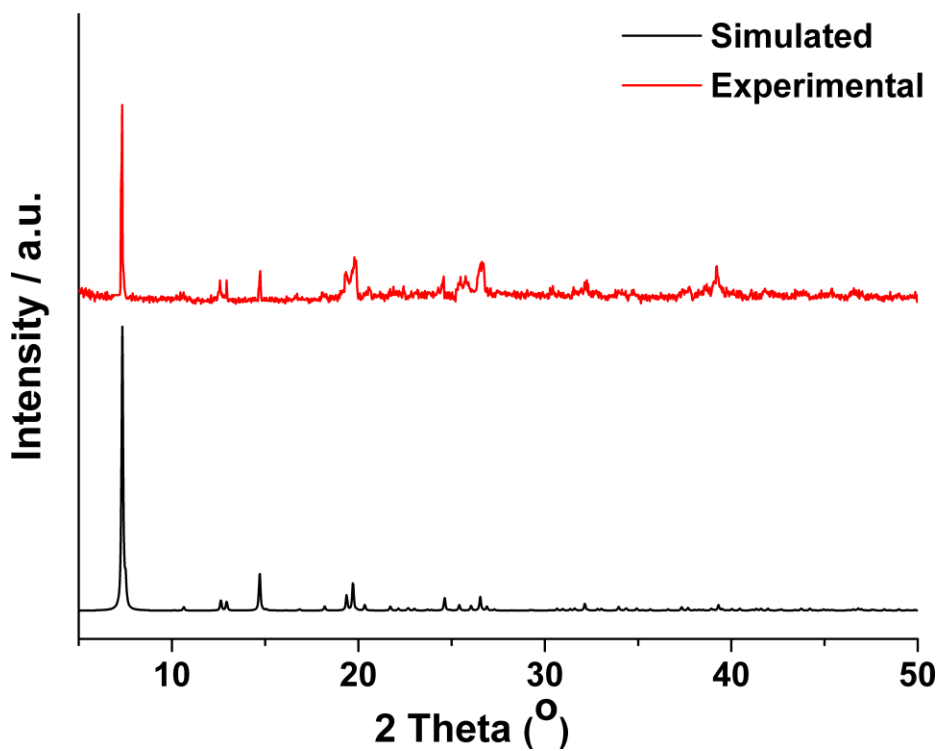


Figure S10. Simulated and experimental PXRD pattern of **5** (black and red respectively).

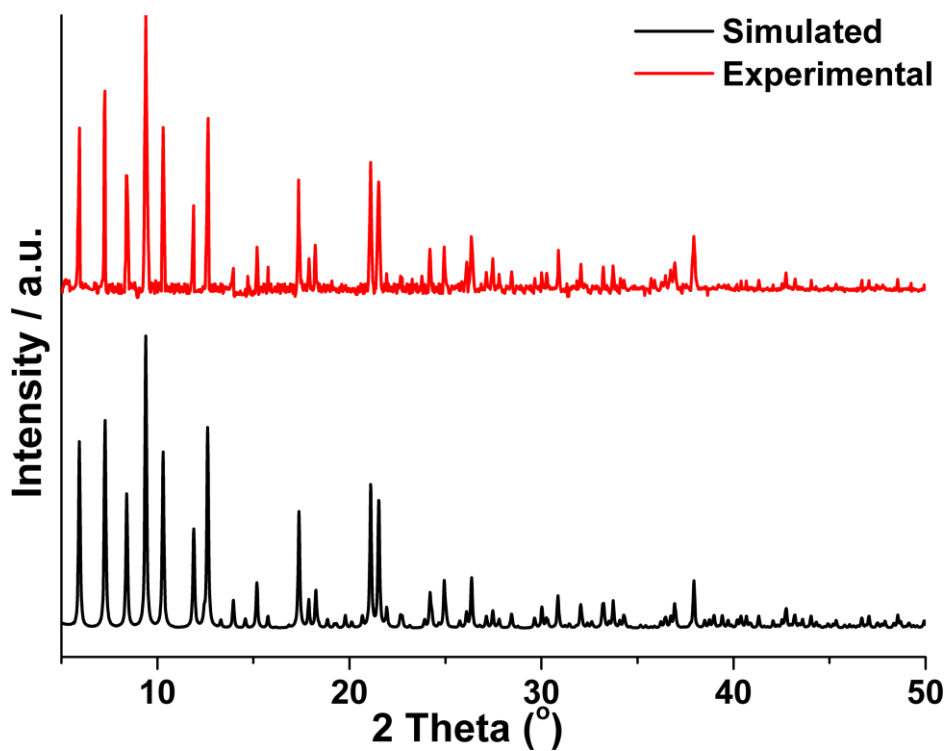


Figure S11. Simulated and experimental PXRD pattern of **6** (black and red respectively).

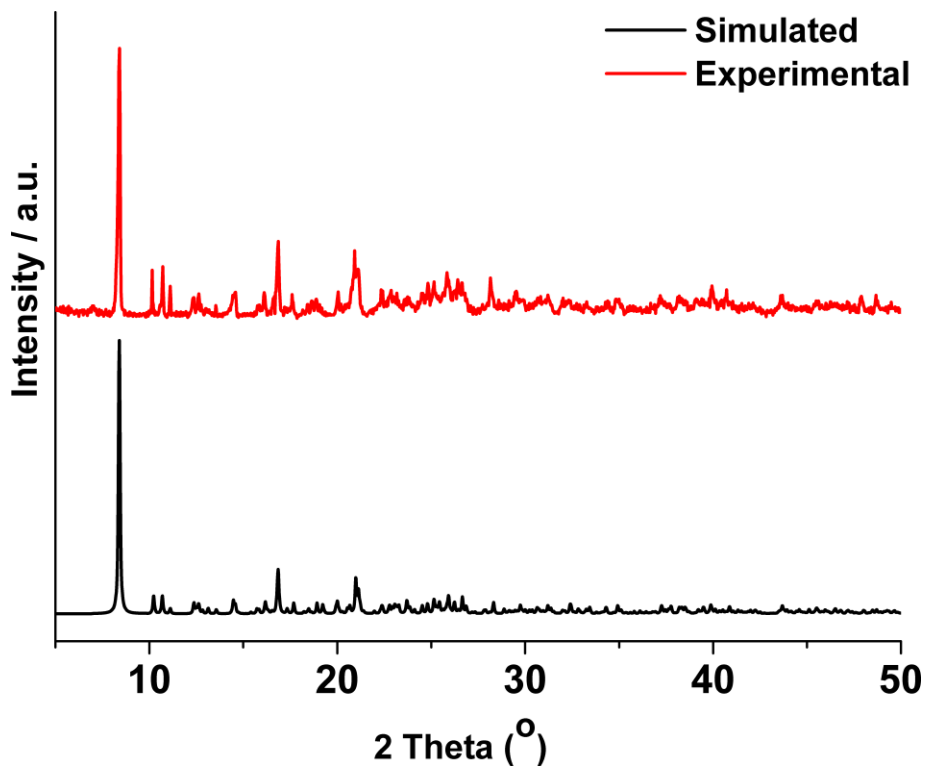


Figure S12. Simulated and experimental PXRD pattern of **7** (black and red respectively).

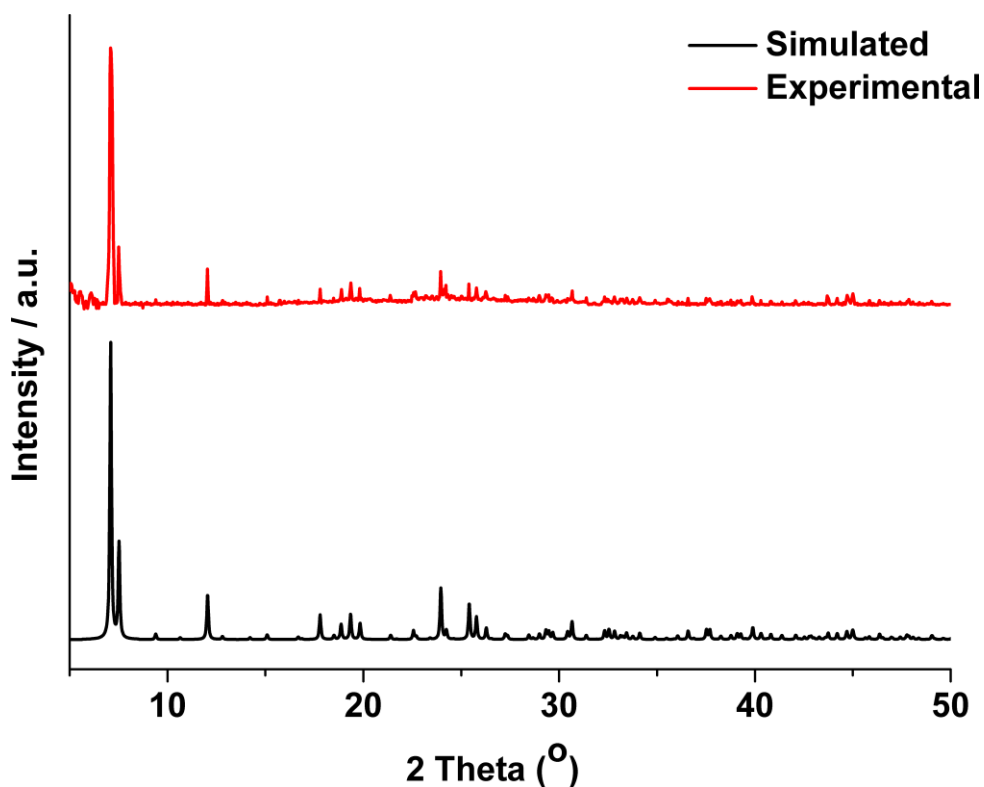


Figure S13. Simulated and experimental PXRD pattern of **8** (black and red respectively).

Table S1. Selected crystal data for 1 - 4.

Compound	1	2	3	4
CCDC No	2033666	2033667	2033668	2033669
Chemical formula	C ₇₈ H ₁₀₀ Ca ₄ N ₁₄ O ₂₇	C ₃₃ H ₃₆ Sr ₂ N ₅ O ₁₂	C ₃₆ H ₄₂ Ba ₂ N ₆ O ₁ 2	C ₁₂₀ H ₁₃₂ Mg ₈ N ₂ 4O ₄₅
Formula Mass	1826.00	869.90	1025.44	2822.94
Crystal System	Tetragonal	Monoclinic	Monoclinic	Monoclinic
a (Å)	15.619(11)	21.096(5)	22.746 (8)	13.028 (10)
b (Å)	15.619(11)	12.176(3)	8.433 (3),	18.865 (14)
c (Å)	18.827(13)	14.196(3)	22.517 (8)	13.91 (1)
a (deg)	90	90	90	90
β (deg)	90	95.269(6)	118.288(5)	93.925 (17)
γ (deg)	90	90	90	90
Unit Cell Volume (Å ³)	4593 (7)	3631.1(8)	3803 (2)	3410 (2)
Temperature (K)	130	130	130	120
Space group	<i>I4/m</i>	<i>P 2₁/c</i>	<i>P2₁/c</i>	<i>P2₁/c</i>
Z	2	4	4	1
No. of reflections measures	10458	59753	34774	38930
No. of independent reflections	2296	6693	7334	6369
No of observed reflections [I > 2.0σ(I)]	1830	4951	6722	4407
R _{int}	0.025	0.052	0.014	0.066
R[F ² > 2σ(F ²)]	0.065	0.057	0.064	0.056
wR(F ²)	0.105	0.087	0.108	0.071

Table S2. Selected crystal data for 5 - 8.

Compound	5	6	7	8
CCDC No	2033670	2033671	2033672	2033673
Chemical formula	$C_{63}H_{77}Ca_4N_{13}O_{27}$	$C_{528}H_{540}N_{128}O_1$ $83Sr_{24}$	$C_{168}H_{232}Cl_6N_{40}$ $O_{56}Sr_{11}$	$C_{69}H_{79}Ba_5Cl_2$ $N_{15}O_{29}$
Formula Mass	1608.66	13709.54	4884.40	2339.99
Crystal system	Tetragonal	Cubic	Tetragonal	Tetragonal
a (Å)	16.617 (2)	42.0581 (14)	16.8066 (5)	16.604 (3)
b (Å)	16.617 (2)	42.0581 (14)	16.8066 (5)	16.604 (3)
c (Å)	17.448 (3)	42.0581 (14)	17.7945 (7)	18.804 (4)
a (deg)	90	90	90	90
β (deg)	90	90	90	90
γ (deg)	90	90	90	90
Unit Cell Volume (Å ³)	4817.8 (15)	74396 (7)	5026.3 (4)	5184 (2)
Temperature (K)	130	130	120	130
Space group	I4/m	Fm-3c	I4/m	--I4/m
Z	2	4	1	2
No. of reflections measured	10153	45519	12768	14062
No. of independent reflections	2356	3093	2580	2536
No of observed reflections [I > 2.0 σ (I)]	1805	2292	2133	2536

R_{int}	0.018	0.027	0.014	0.038
$R[F2 > 2\sigma(F2)]$	0.052	0.030	0.042	0.041
$wR(F2)$	0.107	0.065	0.068	0.079

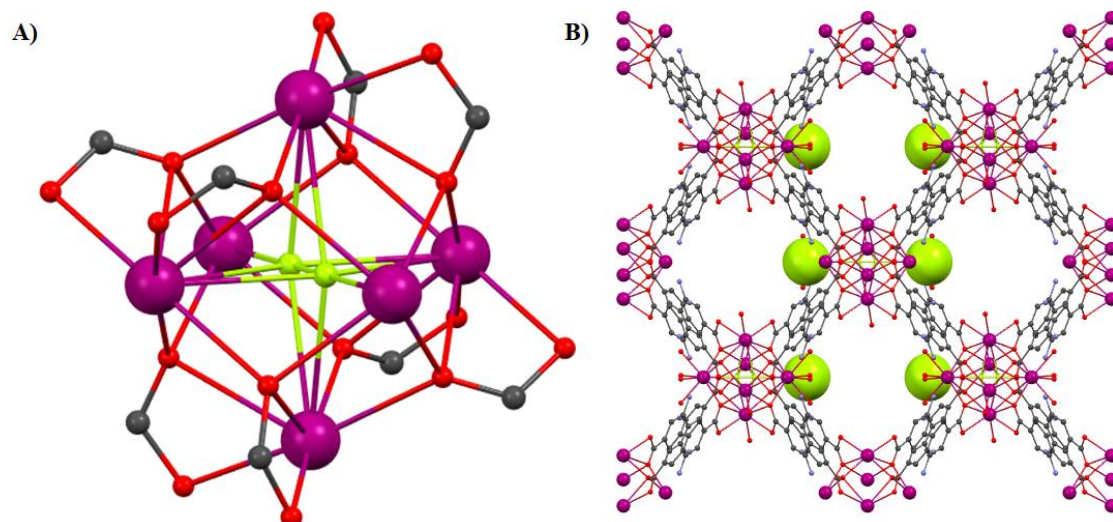


Figure S14. Representation of the SBU and b) 3-D structure along the b axis of 7. H atoms and solvent molecules were omitted for clarity. Colour code: Sr, magenta; C, gray; O, red; N, blue; Cl green.

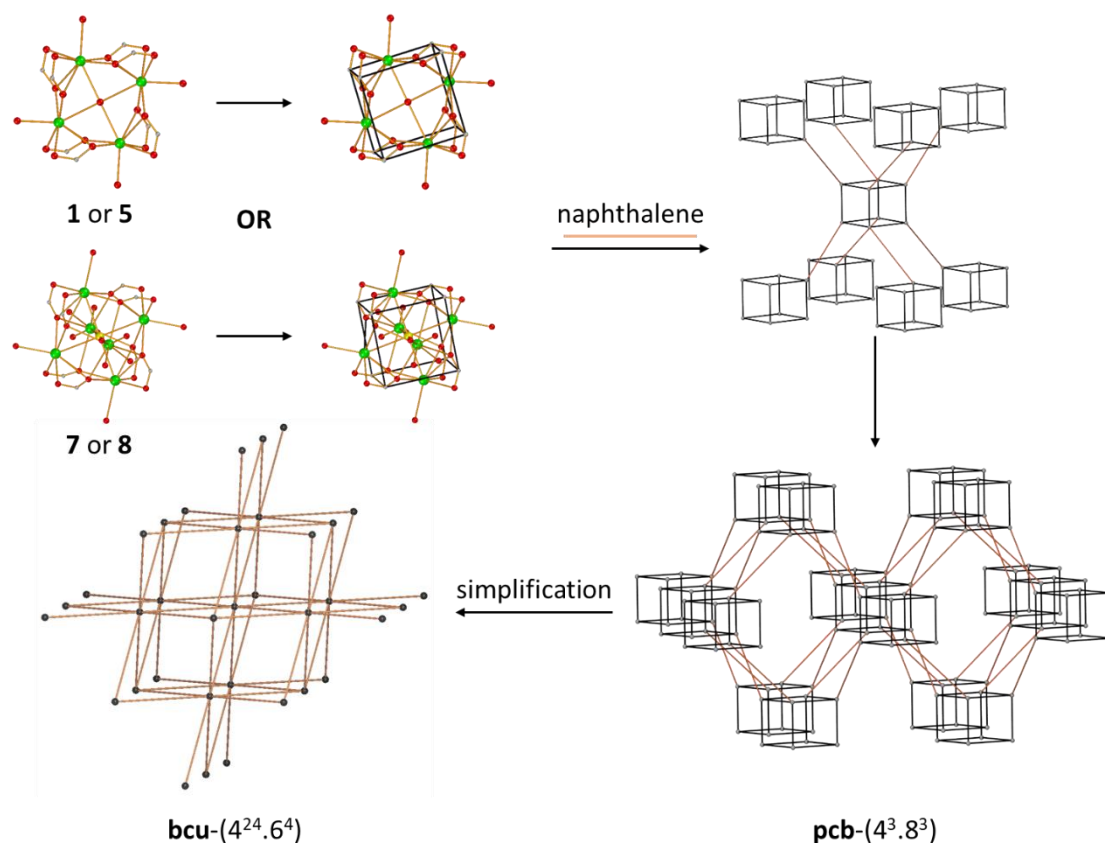


Figure S15. The deconstruction of the frameworks 1, 5, 7 and 8. Color code: Metal green, O red, C grey, Cl yellow.

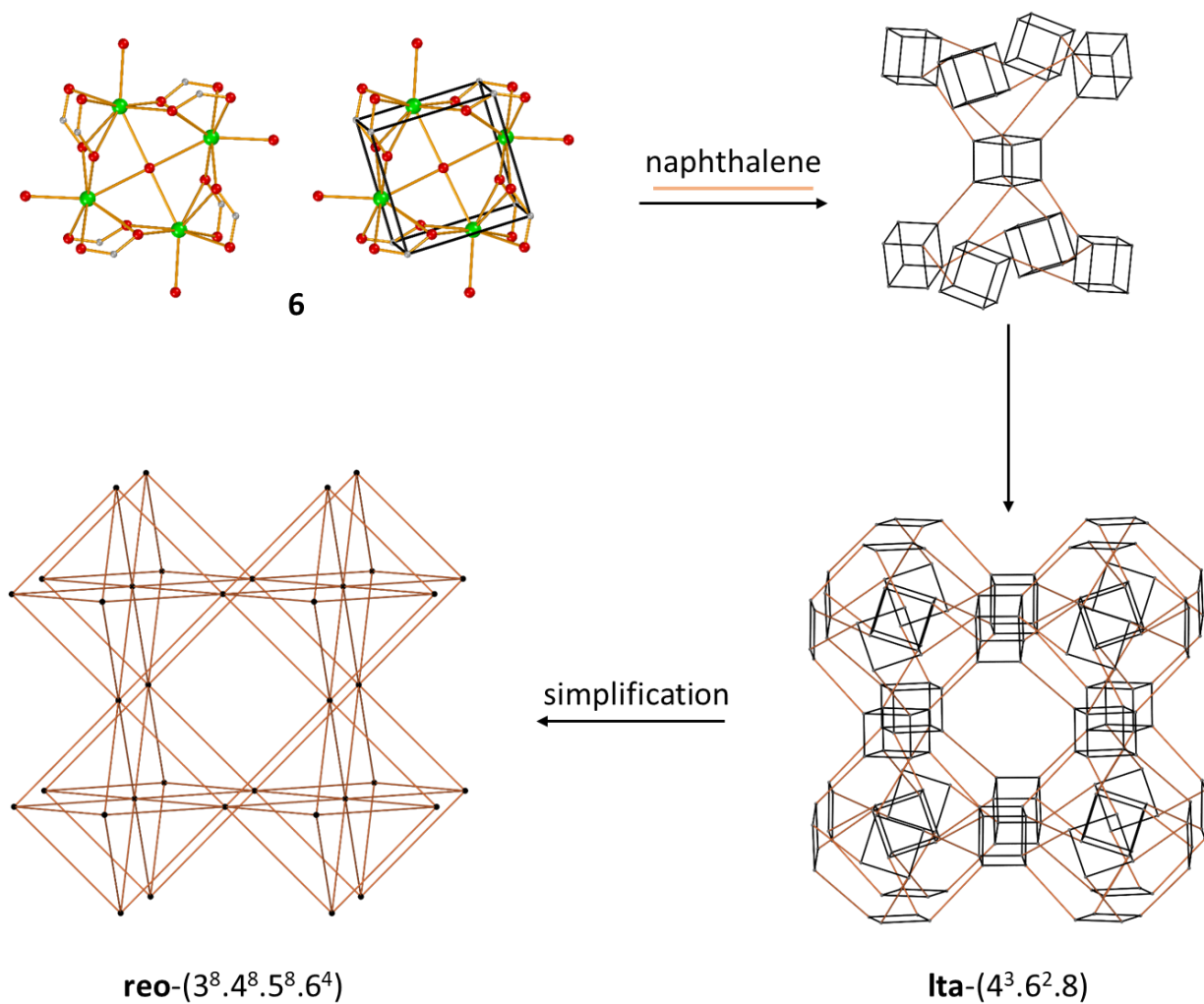


Figure S16. The deconstruction of the frameworks of **6**. Color code: Metal green, O red, C grey.

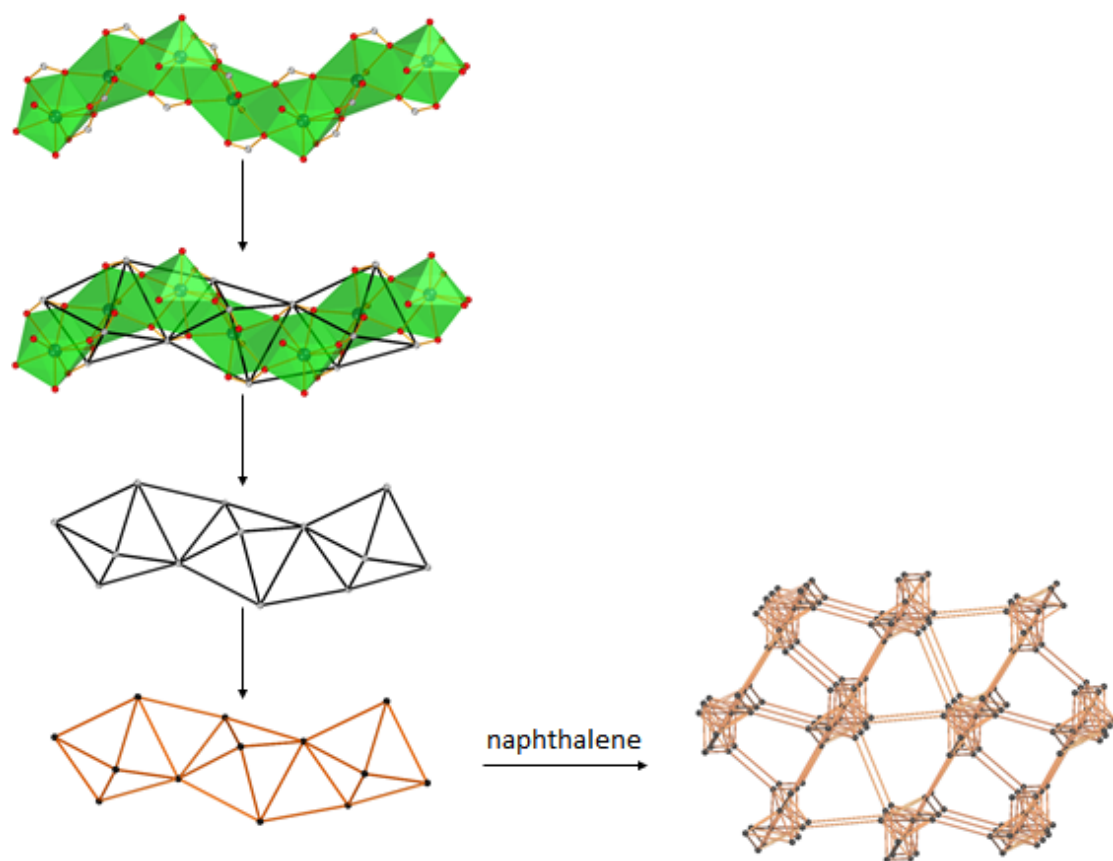


Figure S17. The deconstruction of the framework of **2**. Color code: Metal green, O red, C grey

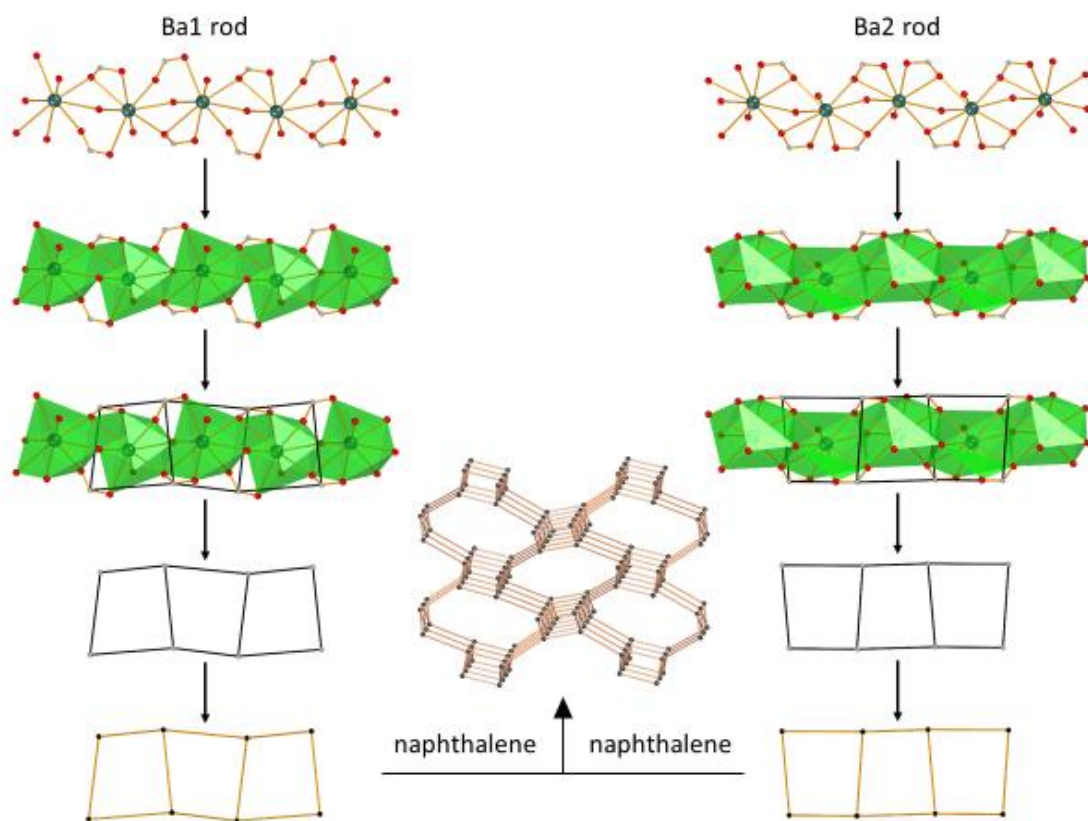


Figure S18. The deconstruction of the framework of **3**. Color code: Metal green, O red, C grey

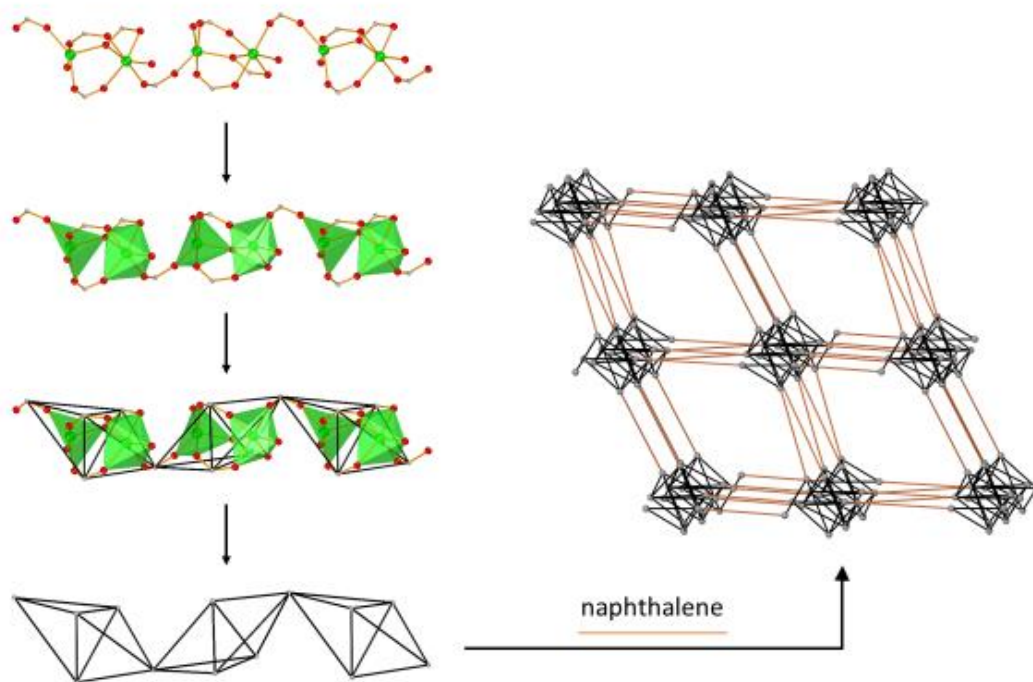


Figure S19. The deconstruction of the framework of **4**. Color code: Metal green, O red, C grey.

Table S3. Selected bond lengths (Å) and angles (°) for 1

Ca1—O1	2.568 (3)	Ca1—O2	2.456 (3)
Ca1—O1 ⁱ	2.568 (3)	Ca1—O2 ⁱ	2.456 (3)
Ca1—O1 ⁱⁱ	2.331 (3)	Ca1—O3	2.5639 (19)
Ca1—O1 ⁱⁱⁱ	2.331 (3)	Ca1—O4	2.332 (4)
O1—Ca1—O1 ⁱ	73.97 (12)	O1 ⁱⁱ —Ca1—O4	88.08 (10)
O1—Ca1—O1 ⁱⁱ	86.64 (11)	O1 ⁱⁱⁱ —Ca1—O2	168.23 (9)
O1—Ca1—O1 ⁱⁱⁱ	137.63 (11)	O1 ⁱⁱⁱ —Ca1—O2 ⁱ	92.31 (9)
O1—Ca1—O2	52.30 (8)	O1 ⁱⁱⁱ —Ca1—O3	70.67 (8)
O1—Ca1—O2 ⁱ	103.92 (9)	O1 ⁱⁱⁱ —Ca1—O4	88.08 (10)
O1—Ca1—O3	67.13 (6)	O2—Ca1—O2 ⁱ	90.17 (13)
O1—Ca1—O4	132.60 (8)	O2—Ca1—O3	118.00 (8)
O1 ⁱ —Ca1—O1 ⁱⁱ	137.63 (10)	O2—Ca1—O4	80.95 (9)
O1 ⁱ —Ca1—O1 ⁱⁱⁱ	86.64 (12)	O2 ⁱ —Ca1—O3	118.00 (8)
O1 ⁱ —Ca1—O2	103.92 (10)	O2 ⁱ —Ca1—O4	80.95 (9)
O1 ⁱ —Ca1—O2 ⁱ	52.30 (8)	O3—Ca1—O4	151.20 (9)
O1 ⁱ —Ca1—O3	67.13 (6)	Ca1—O3—Ca1 ⁱⁱⁱ	90.00 (8)
O1 ⁱ —Ca1—O4	132.60 (8)	Ca1—O3—Ca1 ^{viii}	90.000 (14)
O1 ⁱⁱ —Ca1—O1 ⁱⁱⁱ	83.03 (13)	Ca1—O3—Ca1 ^{ix}	179.996
O1 ⁱⁱ —Ca1—O2	92.31 (9)	Ca1 ⁱⁱⁱ —O3—Ca1 ^{viii}	179.996
O1 ⁱⁱ —Ca1—O2 ⁱ	168.23 (9)	Ca1 ⁱⁱⁱ —O3—Ca1 ^{ix}	90.000 (14)
O1 ⁱⁱ —Ca1—O3	70.67 (8)	Ca1 ^{viii} —O3—Ca1 ^{ix}	90.00 (8)

Symmetry codes: (i) x, y, -z+1; (ii) y, -x+1, z; (iii) y, -x+1, -z+1; (iv) -x+1, -y, z; (v) y+1/2, -x+1/2, -z+1/2; (vi) -y+1/2, x-1/2, -z+1/2; (vii) -x+3/2, -y+3/2, -z+3/2; (viii) -y+1, x, z; (ix) -x+1, -y+1, -z+1; (x) -x+1, -y+1, z

Table S4. Selected bond lengths (Å) and angles (°) for **5**

Ca1—O1	2.4302 (18)	Ca1—O2 ⁱⁱ	2.2516 (19)
Ca1—O1 ⁱ	2.4302 (18)	Ca1—O2 ⁱⁱⁱ	2.2516 (19)
Ca1—O2	2.6591 (19)	Ca1—O3	2.6700 (8)
Ca1—O2 ⁱ	2.6591 (19)	Ca1—O4	2.346 (3)
O1—Ca1—O1 ⁱ	79.43 (10)	O2 ⁱ —Ca1—O2 ⁱⁱ	135.46 (8)
O1—Ca1—O2	51.30 (6)	O2 ⁱ —Ca1—O2 ⁱⁱⁱ	90.47 (10)
O1—Ca1—O2 ⁱ	94.17 (7)	O2 ⁱ —Ca1—O3	65.13 (4)
O1—Ca1—O2 ⁱⁱ	99.71 (7)	O2 ⁱ —Ca1—O4	134.41 (6)
O1—Ca1—O2 ⁱⁱ	173.18 (7)	O2 ⁱⁱ —Ca1—O2 ⁱⁱⁱ	80.32 (10)
O1—Ca1—O3	115.82 (5)	O2 ⁱⁱ —Ca1—O3	70.72 (5)
O1—Ca1—O4	83.88 (7)	O2 ⁱⁱ —Ca1—O4	89.30 (7)
O1 ⁱ —Ca1—O2	94.17 (7)	O2 ⁱⁱⁱ —Ca1—O3	70.72 (5)
O1 ⁱ —Ca1—O2 ⁱ	51.30 (6)	O2 ⁱⁱⁱ —Ca1—O4	89.30 (7)
O1 ⁱ —Ca1—O2 ⁱⁱ	173.18 (7)	O3—Ca1—O4	153.48 (7)
O1 ⁱ —Ca1—O2 ⁱⁱⁱ	99.71 (7)	Ca1—O2—Ca1 ^v	100.18 (7)
O1 ⁱ —Ca1—O3	115.82 (5)	Ca1 ^{vi} —O3—Ca1 ⁱⁱⁱ	90.000 (16)
O1 ⁱ —Ca1—O4	83.88 (7)	Ca1 ^{vi} —O3—Ca1 ^v	90.000 (16)
O2—Ca1—O2 ⁱ	66.20 (9)	Ca1 ⁱⁱⁱ —O3—Ca1 ^v	179.996
O2—Ca1—O2 ⁱⁱ	90.47 (10)	Ca1 ^{vi} —O3—Ca1	179.996
O2—Ca1—O2 ⁱⁱⁱ	135.46 (8)	Ca1 ⁱⁱⁱ —O3—Ca1	90.000 (5)
O2—Ca1—O3	65.13 (4)	Ca1 ^v —O3—Ca1	90.000 (16)
O2—Ca1—O4	134.41 (6)		

Symmetry codes: (i) $x, y, -z$; (ii) $y, -x+1, z$; (iii) $y, -x+1, -z$; (iv) $-x+3/2, -y+3/2, -z+1/2$; (v) $-y+1, x, -z$; (vi) $-x+1, -y+1, -z$; (vii) $-x, -y+1, z$; (viii) $-x, -y+1, -z$.

Table S5. Selected bond lengths (Å) and angles (°) for **7**.

Sr1—Cl1	2.9448 (8)	Sr1—O6 ⁱⁱ	2.661 (5)
Sr1—O1	2.574 (2)	Sr1—O6 ⁱⁱⁱ	2.807 (5)
Sr1—O1 ⁱⁱⁱ	2.574 (2)	Sr2—Cl1 ^{iv}	2.413 (3)
Sr1—O2	2.645 (5)	Sr2—O3	2.496 (4)
Sr1—O2 ⁱ	2.374 (5)	Sr2—O3 ⁱ	2.496 (4)
Sr1—O2 ⁱⁱ	2.374 (5)	Sr2—O3 ^{vi}	2.496 (4)
Sr1—O2 ⁱⁱⁱ	2.645 (5)	Sr2—O3 ^{vii}	2.496 (4)
Sr1—O4	2.514 (4)	Sr2—O6 ⁱⁱ	2.636 (5)
Sr1—O4 ⁱⁱⁱ	2.514 (4)	Sr2—O6 ⁱⁱⁱ	2.636 (5)
Sr1—O6	2.807 (5)	Sr2—O6 ^{iv}	2.636 (5)
Sr1—O6 ⁱ	2.661 (5)	Sr2—O6 ^v	2.636 (5)
O1—Sr1—Cl1	100.23 (8)	O4 ⁱⁱⁱ —Sr1—O6 ⁱ	106.16 (13)
O1—Sr1—O1 ⁱⁱⁱ	99.36 (11)	O4 ⁱⁱⁱ —Sr1—O6 ⁱⁱ	96.39 (13)
O1—Sr1—O2	48.76 (11)	O4 ⁱⁱⁱ —Sr1—O6 ⁱⁱⁱ	124.65 (13)
O1—Sr1—O2 ⁱ	102.12 (13)	O6—Sr1—Cl1	53.43 (10)
O1—Sr1—O2 ⁱⁱ	153.68 (14)	O6—Sr1—O6 ⁱ	73.56 (19)
O1—Sr1—O2 ⁱⁱⁱ	87.52 (13)	O6—Sr1—O6 ⁱⁱ	126.27 (17)
O1—Sr1—O4	76.76 (10)	O6—Sr1—O6 ⁱⁱⁱ	80.2 (2)
O1—Sr1—O4 ⁱⁱⁱ	87.61 (10)	O6 ⁱ —Sr1—Cl1	54.72 (11)
O1—Sr1—O6	49.12 (11)	O6 ⁱ —Sr1—O6 ⁱⁱ	85.6 (2)
O1—Sr1—O6 ⁱ	87.50 (12)	O6 ⁱ —Sr1—O6 ⁱⁱⁱ	126.27 (17)
O1—Sr1—O6 ⁱⁱ	172.72 (11)	O6 ⁱⁱ —Sr1—Cl1	73.93 (11)
O1—Sr1—O6 ⁱⁱⁱ	109.11 (11)	O6 ⁱⁱ —Sr1—O6 ⁱⁱⁱ	73.56 (19)
O1 ⁱⁱⁱ —Sr1—Cl1	121.02 (7)	O6 ⁱⁱⁱ —Sr1—Cl1	71.91 (11)
O1 ⁱⁱⁱ —Sr1—O2	87.52 (13)	O3—Sr2—Cl1 ^{iv}	131.16 (9)
O1 ⁱⁱⁱ —Sr1—O2 ⁱ	153.68 (14)	O3—Sr2—O3 ⁱ	64.33 (10)
O1 ⁱⁱⁱ —Sr1—O2 ⁱⁱ	102.12 (13)	O3—Sr2—O3 ^{vi}	97.67 (18)
O1 ⁱⁱⁱ —Sr1—O2 ⁱⁱⁱ	48.76 (11)	O3—Sr2—O3 ^{vii}	64.33 (10)
O1 ⁱⁱⁱ —Sr1—O4	87.61 (10)	O3—Sr2—O6 ⁱⁱ	75.71 (13)

O1 ⁱⁱⁱ —Sr1—O4 ⁱⁱⁱ	76.76 (10)	O3—Sr2—O6 ⁱⁱⁱ	131.67 (13)
O1 ⁱⁱⁱ —Sr1—O6	109.11 (11)	O3—Sr2—O6 ^{iv}	87.89 (13)
O1 ⁱⁱⁱ —Sr1—O6 ⁱ	172.72 (11)	O3—Sr2—O6 ^v	151.04 (13)
O1 ⁱⁱⁱ —Sr1—O6 ⁱⁱ	87.50 (12)	O3 ⁱ —Sr2—Cl1 ^{iv}	131.16 (9)
O1 ⁱⁱⁱ —Sr1—O6 ⁱⁱⁱ	49.12 (11)	O3 ⁱ —Sr2—O3 ^{vi}	64.33 (10)
O2—Sr1—Cl1	66.49 (11)	O3 ⁱ —Sr2—O3 ^{vii}	97.67 (18)
O2—Sr1—O2 ⁱ	118.2 (3)	O3 ⁱ —Sr2—O6 ⁱⁱ	131.67 (13)
O2—Sr1—O2 ⁱⁱ	146.7 (2)	O3 ⁱ —Sr2—O6 ⁱⁱⁱ	151.04 (13)
O2—Sr1—O2 ⁱⁱⁱ	47.7 (2)	O3 ⁱ —Sr2—O6 ^{iv}	75.71 (13)
O2—Sr1—O4	123.44 (14)	O3 ⁱ —Sr2—O6 ^v	87.89 (13)
O2—Sr1—O4 ⁱⁱⁱ	130.57 (14)	O3 ^{vi} —Sr2—Cl1 ^{iv}	131.16 (9)
O2—Sr1—O6	21.71 (13)	O3 ^{vi} —Sr2—O3 ^{vii}	64.33 (10)
O2—Sr1—O6 ⁱ	95.27 (18)	O3 ^{vi} —Sr2—O6 ⁱⁱ	151.04 (13)
O2—Sr1—O6 ⁱⁱ	129.84 (14)	O3 ^{vi} —Sr2—O6 ⁱⁱⁱ	87.89 (13)
O2—Sr1—O6 ⁱⁱⁱ	65.87 (16)	O3 ^{vi} —Sr2—O6 ^{iv}	131.67 (13)
O2 ⁱ —Sr1—Cl1	69.68 (12)	O3 ^{vi} —Sr2—O6 ^v	75.71 (13)
O2 ⁱ —Sr1—O2 ⁱⁱ	53.5 (3)	O3 ^{vii} —Sr2—Cl1 ^{iv}	131.16 (9)
O2 ⁱ —Sr1—O2 ⁱⁱⁱ	146.7 (2)	O3 ^{vii} —Sr2—O6 ⁱⁱ	87.89 (13)
O2 ⁱ —Sr1—O4	82.72 (15)	O3 ^{vii} —Sr2—O6 ⁱⁱⁱ	75.71 (13)
O2 ⁱ —Sr1—O4 ⁱⁱⁱ	89.08 (16)	O3 ^{vii} —Sr2—O6 ^{iv}	151.04 (13)
O2 ⁱ —Sr1—O6	96.46 (19)	O3 ^{vii} —Sr2—O6 ^v	131.67 (13)
O2 ⁱ —Sr1—O6 ⁱ	22.91 (14)	O6 ⁱⁱ —Sr2—Cl1 ^{iv}	61.50 (10)
O2 ⁱ —Sr1—O6 ⁱⁱ	71.95 (17)	O6 ⁱⁱ —Sr2—O6 ⁱⁱⁱ	76.84 (9)
O2 ⁱ —Sr1—O6 ⁱⁱⁱ	133.80 (15)	O6 ⁱⁱ —Sr2—O6 ^{iv}	76.84 (9)
O2 ⁱⁱ —Sr1—Cl1	81.50 (12)	O6 ⁱⁱ —Sr2—O6 ^v	123.0 (2)
O2 ⁱⁱ —Sr1—O2 ⁱⁱⁱ	118.2 (3)	O6 ⁱⁱⁱ —Sr2—Cl1 ^{iv}	61.50 (10)
O2 ⁱⁱ —Sr1—O4	89.08 (16)	O6 ⁱⁱⁱ —Sr2—O6 ^{iv}	123.0 (2)
O2 ⁱⁱ —Sr1—O4 ⁱⁱⁱ	82.72 (15)	O6 ⁱⁱⁱ —Sr2—O6 ^v	76.84 (9)
O2 ⁱⁱ —Sr1—O6	133.80 (15)	O6 ^{iv} —Sr2—Cl1 ^{iv}	61.50 (10)
O2 ⁱⁱ —Sr1—O6 ⁱ	71.95 (17)	O6 ^{iv} —Sr2—O6 ^v	76.84 (9)

O2 ⁱⁱ —Sr1—O6 ⁱⁱ	22.91 (14)	O6 ^v —Sr2—Cl1 ^{iv}	61.50 (10)
O2 ⁱⁱ —Sr1—O6 ⁱⁱⁱ	96.46 (19)	Sr2 ^{iv} —Cl1—Sr1	102.80 (6)
O2 ⁱⁱⁱ —Sr1—Cl1	77.29 (11)	Sr2 ^{iv} —Cl1—Sr1 ⁱ	102.80 (6)
O2 ⁱⁱⁱ —Sr1—O4	130.57 (14)	Sr1—Cl1—Sr1 ⁱ	87.19 (3)
O2 ⁱⁱⁱ —Sr1—O4 ⁱⁱⁱ	123.44 (14)	Sr2 ^{iv} —Cl1—Sr1 ^{iv}	102.80 (6)
O2 ⁱⁱⁱ —Sr1—O6	65.87 (16)	Sr1—Cl1—Sr1 ^{iv}	154.41 (13)
O2 ⁱⁱⁱ —Sr1—O6 ⁱ	129.84 (14)	Sr1 ⁱ —Cl1—Sr1 ^{iv}	87.19 (3)
O2 ⁱⁱⁱ —Sr1—O6 ⁱⁱ	95.27 (18)	Sr2 ^{iv} —Cl1—Sr1 ^v	102.80 (6)
O2 ⁱⁱⁱ —Sr1—O6 ⁱⁱⁱ	21.71 (13)	Sr1—Cl1—Sr1 ^v	87.19 (3)
O4—Sr1—Cl1	151.10 (10)	Sr1 ⁱ —Cl1—Sr1 ^v	154.41 (13)
O4—Sr1—O4 ⁱⁱⁱ	14.11 (17)	Sr1 ^{iv} —Cl1—Sr1 ^v	87.19 (3)
O4—Sr1—O6 ⁱ	96.39 (13)	Sr1 ^v —O2—Sr1	107.92 (17)
O4—Sr1—O6 ⁱⁱ	106.16 (13)	Sr1—O6—Sr1 ^v	95.89 (15)
O4—Sr1—O6 ⁱⁱⁱ	136.62 (13)	Sr1—O6—Sr2 ^{iv}	100.97 (14)
O4 ⁱⁱⁱ —Sr1—Cl1	158.42 (10)	Sr1 ^v —O6—Sr2 ^{iv}	104.91 (16)
O4 ⁱⁱⁱ —Sr1—O6	136.62 (13)		

Symmetry codes: (i) $-y+1, x, z$; (ii) $-y+1, x, -z+1$; (iii) $x, y, -z+1$; (iv) $-x+1, -y+1, -z+1$; (v) $y, -x+1, -z+1$; (vi) $-x+1, -y+1, z$; (vii) $y, -x+1, z$; (viii) $-x+3/2, -y+1/2, -z+1/2$.

Table S6. Selected bond lengths (Å) and angles (°) for **8**

Ba1—O1	2.627 (4)	Ba2—O2	3.132 (5)
Ba1—O1 ⁱ	2.627 (4)	Ba2—O2 ⁱⁱⁱ	3.132 (5)
Ba1—O2	2.883 (4)	Ba2—O2 ^{iv}	3.132 (5)
Ba1—O2 ⁱ	2.883 (4)	Ba2—O2 ^v	3.132 (5)
Ba1—O2 ⁱⁱ	2.713 (6)	Ba2—O4	2.651 (19)
Ba1—O2 ⁱⁱⁱ	2.665 (4)	Ba2—O4 ⁱⁱⁱ	2.651 (19)
Ba1—O3	2.665 (4)	Ba2—O4 ^{iv}	2.651 (19)
Ba1—Cl1	3.1228 (7)	Ba2—O4 ^v	2.651 (19)
O1—Ba1—Cl1	107.04 (10)	O2 ⁱⁱⁱ —Ba1—Cl1	65.72 (8)
O1—Ba1—O1 ⁱ	101.0 (2)	O2 ⁱⁱⁱ —Ba2—O2 ^{iv}	121.52 (15)
O1—Ba1—O2	46.18 (12)	O2 ⁱⁱⁱ —Ba2—O2 ^v	76.20 (7)
O1—Ba1—O2 ⁱ	99.26 (12)	O2 ⁱⁱⁱ —Ba2—O4	109.9 (4)
O1—Ba1—O2 ⁱⁱ	165.99 (13)	O2 ⁱⁱⁱ —Ba2—O4 ⁱⁱⁱ	93.3 (4)
O1—Ba1—O2 ⁱⁱⁱ	92.71 (14)	O2 ⁱⁱⁱ —Ba2—O4 ^{iv}	144.7 (4)
O1—Ba1—O3	92.86 (13)	O2 ⁱⁱⁱ —Ba2—O4 ^v	122.2 (4)
O1 ⁱ —Ba1—Cl1	107.04 (10)	O2 ^{iv} —Ba2—O2 ^v	76.20 (7)
O1 ⁱ —Ba1—O2	99.26 (12)	O2 ^{iv} —Ba2—O4	122.2 (4)
O1 ⁱ —Ba1—O2 ⁱ	46.18 (12)	O2 ^{iv} —Ba2—O4 ⁱⁱⁱ	144.7 (4)
O1 ⁱ —Ba1—O2 ⁱⁱ	92.71 (14)	O2 ^{iv} —Ba2—O4 ^{iv}	93.3 (4)
O1 ⁱ —Ba1—O2 ⁱⁱⁱ	165.99 (13)	O2 ^{iv} —Ba2—O4 ^v	109.9 (4)
O1 ⁱ —Ba1—O3	92.86 (13)	O2 ^v —Ba2—O4	144.7 (4)
O2—Ba1—Cl1	63.44 (8)	O2 ^v —Ba2—O4 ⁱⁱⁱ	109.9 (4)
O2—Ba1—O2 ⁱ	67.12 (16)	O2 ^v —Ba2—O4 ^{iv}	122.2 (4)
O2—Ba1—O2 ⁱⁱ	129.08 (15)	O2 ^v —Ba2—O4 ^v	93.3 (4)
O2—Ba1—O2 ⁱⁱⁱ	88.25 (18)	O4—Ba2—O4 ⁱⁱⁱ	37.0 (5)
O2—Ba1—O3	138.72 (11)	O4—Ba2—O4 ^{iv}	37.0 (5)
O2 ⁱ —Ba1—Cl1	63.44 (8)	O4—Ba2—O4 ^v	53.3 (8)
O2 ⁱ —Ba1—O2 ⁱⁱ	88.25 (18)	O4 ^{iv} —Ba2—O4 ⁱⁱⁱ	53.3 (8)
O2 ⁱ —Ba1—O2 ⁱⁱⁱ	129.08 (15)	O4 ⁱⁱⁱ —Ba2—O4 ^{iv}	53.3 (8)

O2 ⁱ —Ba1—O3	138.72 (11)	O4 ⁱⁱⁱ —Ba2—O4 ^v	37.0 (5)
O2 ⁱⁱ —Ba1—Cl1	65.72 (8)	O4 ^{iv} —Ba2—O4 ^v	37.0 (5)
O2 ⁱⁱ —Ba1—O2 ⁱⁱⁱ	73.44 (18)	Ba1—Cl1—Ba1 ^{iv}	90.000
O2 ⁱⁱ —Ba1—O3	89.14 (15)	Ba1—Cl1—Ba1 ^x	179.996
O2 ⁱⁱⁱ —Ba1—Cl1	65.72 (8)	Ba1 ^{iv} —Cl1—Ba1 ^x	90.000
O2 ⁱⁱⁱ —Ba1—O3	89.14 (15)	Ba1—Cl1—Ba1 ⁱⁱ	90.000
O3—Ba1—Cl1	148.07 (15)	Ba1 ^{iv} —Cl1—Ba1 ⁱⁱ	179.996
O2—Ba2—O2 ⁱⁱⁱ	76.20 (7)	Ba1 ^x —Cl1—Ba1 ⁱⁱ	90.000
O2—Ba2—O2 ^{iv}	76.20 (7)	Ba2—O2—Ba1	94.40 (11)
O2—Ba2—O2 ^v	121.52 (15)	Ba2—O2—Ba1 ^{xi}	98.94 (13)
O2—Ba2—O4	93.3 (4)	Ba1—O2—Ba1 ^{xi}	105.45 (13)
O2—Ba2—O4 ⁱⁱⁱ	122.2 (4)	O2—Ba2—O4 ^{iv}	109.9 (4)
O2—Ba2—O4 ^v	144.7 (4)		

Symmetry codes: (i) $x, y, -z$; (ii) $-y+1, x-1, -z$; (iii) $-y+1, x-1, z$; (iv) $y+1, -x+1, z$; (v) $-x+2, -y, z$; (vi) $-x, -y, -z+1$; (vii) $-y, x, z$; (viii) $y, -x, z$; (ix) $-x+3/2, -y+1/2, -z+1/2$; (x) $-x+2, -y, -z$; (xi) $y+1, -x+1, -z$.

Table S7. Selected bond lengths (Å) and angles (°) for **6**

Sr1—O1	2.6258 (16)	Sr1—O2 ⁱⁱ	2.4745 (18)
Sr1—O1 ⁱⁱⁱ	2.6258 (16)	Sr1—O2 ⁱⁱⁱ	2.6609 (19)
Sr1—O2	2.6609 (19)	Sr1—O3	2.6969 (4)
Sr1—O2 ⁱ	2.4745 (18)	Sr1—O4	2.503 (3)
O1—Sr1—O1 ⁱⁱⁱ	98.11 (8)	O2 ⁱ —Sr1—O2 ⁱⁱ	76.91 (10)
O2—Sr1—O1	49.02 (5)	O2 ⁱ —Sr1—O2 ⁱⁱⁱ	143.26 (8)
O1—Sr1—O2 ⁱ	90.80 (6)	O2 ⁱ —Sr1—O3	73.07 (5)
O1—Sr1—O2 ⁱⁱ	162.43 (7)	O2 ⁱ —Sr1—O4	87.99 (7)
O1—Sr1—O2 ⁱⁱⁱ	102.58 (6)	O2 ⁱⁱ —Sr1—O2 ⁱⁱⁱ	94.71 (10)
O1—Sr1—O3	115.67 (4)	O2 ⁱⁱ —Sr1—O3	73.07 (5)
O1—Sr1—O4	78.96 (6)	O2 ⁱⁱ —Sr1—O4	87.99 (7)
O1 ⁱⁱⁱ —Sr1—O2	102.58 (6)	O2 ⁱⁱⁱ —Sr1—O3	70.28 (4)
O1 ⁱⁱⁱ —Sr1—O2 ⁱ	162.43 (7)	O2 ⁱⁱⁱ —Sr1—O4	127.89 (6)
O1 ⁱⁱⁱ —Sr1—O2 ⁱⁱ	90.80 (6)	O3—Sr1—O4	155.60 (7)
O1 ⁱⁱⁱ —Sr1—O2 ⁱⁱⁱ	49.02 (5)	Sr1—O2—Sr1 ^{vii}	95.85 (6)
O1 ⁱⁱⁱ —Sr1—O3	115.67 (4)	Sr1—O3—Sr1 ^{vii}	90.000 (4)
O1 ⁱⁱⁱ —Sr1—O4	78.96 (6)	Sr1—O3—Sr1 ^{viii}	179.996
O2—Sr1—O2 ⁱ	94.71 (10)	Sr1 ^{vii} —O3—Sr1 ^{viii}	90.000 (4)
O2—Sr1—O2 ⁱⁱ	143.26 (8)	Sr1—O3—Sr1 ⁱⁱ	90.000
O2—Sr1—O2 ⁱⁱⁱ	70.66 (8)	Sr1 ^{vii} —O3—Sr1 ⁱⁱ	179.996
O2—Sr1—O3	70.28 (4)	Sr1 ^{viii} —O3—Sr1 ⁱⁱ	90.000 (4)
O2—Sr1—O4	127.89 (6)		

Symmetry codes: (i) $y, -x+1/2, z$; (ii) $y, -x+1/2, -z+1$; (iii) $x, y, -z+1$; (iv) y, z, x ; (v) z, x, y ; (vi) $-x+1/2, z, y$; (vii) $-y+1/2, x, z$; (viii) $-x+1/2, -y+1/2, -z+1$; (ix) $-x+1/2, y, -z+1/2$; (x) $z, y, -x+1/2$; (xi) $-z+1/2, y, x$.

Table S8. Selected bond lengths (Å) and angles (°) for **2**

Sr1—O1	2.496 (4)	Sr2—O1	2.724 (4)
Sr1—O3 ⁱⁱ	2.669 (4)	Sr2—O2	2.562 (4)
Sr1—O4 ⁱⁱ	2.746 (4)	Sr2—O3 ^{iv}	2.565 (4)
Sr1—O5	2.623 (3)	Sr2—O4 ⁱⁱ	2.589 (3)
Sr1—O6	2.602 (4)	Sr2—O5 ⁱⁱⁱ	2.523 (3)
Sr1—O8 ⁱ	2.526 (4)	Sr2—O7	2.589 (4)
Sr1—O9	2.545 (4)	Sr2—O8	2.816 (4)
Sr1—O11	2.593 (5)	Sr2—O10	2.510 (4)
O1—Sr1—O3 ⁱⁱ	115.61 (12)	O1—Sr2—O3 ^{iv}	127.52 (12)
O1—Sr1—O4 ⁱⁱ	70.17 (11)	O1—Sr2—O4 ⁱⁱ	69.22 (12)
O1—Sr1—O5	126.93 (13)	O1—Sr2—O5 ⁱⁱⁱ	153.53 (12)
O1—Sr1—O6	80.97 (13)	O1—Sr2—O7	85.29 (13)
O1—Sr1—O8 ⁱ	162.72 (14)	O1—Sr2—O8	132.83 (13)
O1—Sr1—O9	85.67 (14)	O1—Sr2—O10	76.96 (15)
O1—Sr1—O11	82.65 (14)	O2—Sr2—O3 ^{iv}	80.26 (12)
O3 ⁱⁱ —Sr1—O4 ⁱⁱ	47.20 (10)	O2—Sr2—O4 ⁱⁱ	115.89 (12)
O3 ⁱⁱ —Sr1—O5	68.99 (12)	O2—Sr2—O5 ⁱⁱⁱ	149.88 (14)
O3 ⁱⁱ —Sr1—O6	102.22 (15)	O2—Sr2—O7	85.43 (16)
O3 ⁱⁱ —Sr1—O8 ⁱ	75.48 (13)	O2—Sr2—O8	117.49 (16)
O3 ⁱⁱ —Sr1—O9	92.57 (14)	O2—Sr2—O10	88.41 (16)
O3 ⁱⁱ —Sr1—O11	158.30 (13)	O3 ^{iv} —Sr2—O4 ⁱⁱ	163.11 (11)
O4 ⁱⁱ —Sr1—O5	105.84 (13)	O3 ^{iv} —Sr2—O5 ⁱⁱⁱ	72.19 (12)
O4 ⁱⁱ —Sr1—O6	107.55 (15)	O3 ^{iv} —Sr2—O7	99.63 (13)
O4 ⁱⁱ —Sr1—O8 ⁱ	115.98 (13)	O3 ^{iv} —Sr2—O8	72.35 (12)
O4 ⁱⁱ —Sr1—O9	76.91 (13)	O3 ^{iv} —Sr2—O10	97.46 (15)
O4 ⁱⁱ —Sr1—O11	143.03 (14)	O4 ⁱⁱ —Sr2—O5 ⁱⁱⁱ	92.86 (12)
O5—Sr1—O6	48.70 (12)	O4 ⁱⁱ —Sr2—O7	77.89 (13)
O5—Sr1—O8 ⁱ	68.49 (13)	O4 ⁱⁱ —Sr2—O8	94.57 (12)
O5—Sr1—O9	146.76 (13)	O4 ⁱⁱ —Sr2—O10	88.34 (15)
O5—Sr1—O11	110.52 (15)	O5 ⁱⁱⁱ —Sr2—O7	110.62 (13)
O6—Sr1—O8 ⁱ	110.59 (15)	O5 ⁱⁱⁱ —Sr2—O8	65.50 (13)

O6—Sr1—O9	163.29 (15)	O5 ⁱⁱⁱ —Sr2—O10	83.42 (14)
O6—Sr1—O11	91.80 (16)	O7—Sr2—O8	47.59 (12)
O8 ⁱ —Sr1—O11	84.15 (14)	O7—Sr2—O10	160.56 (15)
O8 ⁱ —Sr1—O9	80.43 (14)	O8—Sr2—O10	148.88 (14)
O9—Sr1—O11	76.49 (15)	Sr2—O1—Sr1	110.46 (14)
O1—Sr2—O2	47.83 (12)		

Symmetry codes: (i) $x, -y+3/2, z-1/2$; (ii) $x, y+1, z$; (iii) $x, -y+3/2, z+1/2$; (iv) $x, -y+1/2, z+1/2$; (v) $-x+1, -y+1, -z$; (vi) $-x, -y+2, -z+1$; (vii) $x, -y+1/2, z-1/2$; (viii) $x, y-1, z$.

Table S9. Selected bond lengths (Å) and angles (°) for **3**

Ba1—O2	2.663 (5)	Ba2—O3	2.660 (5)
Ba1—O2 ⁱ	2.981 (5)	Ba2—O3 ⁱⁱⁱ	2.865 (5)
Ba1—O7 ⁱ	2.737 (5)	Ba2—O4 ⁱⁱⁱ	2.785 (6)
Ba1—O8	2.782 (5)	Ba2—O5 ^v	2.933 (5)
Ba1—O8 ⁱ	2.881 (5)	Ba2—O5 ^{vi}	2.707 (5)
Ba1—O9	2.818 (6)	Ba2—O6 ^v	2.694 (5)
Ba1—O9 ⁱⁱ	2.927 (6)	Ba2—O11	2.813 (6)
Ba1—O10	2.814 (6)	Ba2—O12	2.831 (6)
O2—Ba1—O2 ⁱ	148.19 (14)	Ba2—O12 ^{iv}	2.893 (6)
O2—Ba1—O7 ⁱ	81.7 (2)	O3—Ba2—O12	118.05 (16)
O2—Ba1—O8	70.30 (15)	O3—Ba2—O12 ^{iv}	63.75 (17)
O2—Ba1—O8 ⁱ	93.86 (15)	O4 ⁱⁱⁱ —Ba2—O3 ⁱⁱⁱ	45.66 (15)
O2—Ba1—O9	85.99 (17)	O3 ⁱⁱⁱ —Ba2—O5 ^v	123.34 (15)
O2—Ba1—O9 ⁱⁱ	67.77 (18)	O3 ⁱⁱⁱ —Ba2—O5 ^{vi}	72.81 (15)
O2—Ba1—O10	133.09 (19)	O3 ⁱⁱⁱ —Ba2—O6 ^v	93.28 (16)
O2 ⁱ —Ba1—O7 ⁱ	96.13 (18)	O11—Ba2—O3 ⁱⁱⁱ	121.33 (16)
O2 ⁱ —Ba1—O8	122.24 (15)	O12—Ba2—O3 ⁱⁱⁱ	62.12 (16)
O2 ⁱ —Ba1—O8 ⁱ	64.66 (14)	O3 ⁱⁱⁱ —Ba2—O12 ^{iv}	106.86 (16)
O2 ⁱ —Ba1—O9	65.13 (16)	O4 ⁱⁱⁱ —Ba2—O5 ^v	83.78 (16)
O2 ⁱ —Ba1—O9 ⁱⁱ	142.43 (16)	O4 ⁱⁱⁱ —Ba2—O5 ^{vi}	97.64 (17)
O2 ⁱ —Ba1—O10	76.45 (18)	O4 ⁱⁱⁱ —Ba2—O6 ^v	78.78 (18)
O8—Ba1—O7 ⁱ	140.62 (17)	O11—Ba2—O4 ⁱⁱⁱ	145.12 (18)
O7 ⁱ —Ba1—O8 ⁱ	44.68 (15)	O12—Ba2—O4 ⁱⁱⁱ	106.98 (17)
O7 ⁱ —Ba1—O9	111.49 (18)	O4 ⁱⁱⁱ —Ba2—O12 ^{iv}	68.48 (17)
O7 ⁱ —Ba1—O9 ⁱⁱ	74.57 (16)	O5 ^v —Ba2—O5 ^{vi}	151.81 (12)
O7 ⁱ —Ba1—O10	78.58 (19)	O6 ^v —Ba2—O5 ^v	45.31 (15)
O8—Ba1—O8 ⁱ	158.45 (3)	O11—Ba2—O5 ^v	83.46 (17)
O8—Ba1—O9	94.03 (16)	O12—Ba2—O5 ^v	140.14 (16)
O8—Ba1—O9 ⁱⁱ	69.51 (15)	O12 ^{iv} —Ba2—O5 ^v	62.83 (16)

O8—Ba1—O10	100.54 (17)	O6 ^v —Ba2—O5 ^{vi}	162.62 (16)
O8 ⁱ —Ba1—O9	69.69 (16)	O11—Ba2—O5 ^{vi}	108.69 (18)
O8 ⁱ —Ba1—O9 ⁱⁱ	118.95 (14)	O12—Ba2—O5 ^{vi}	66.46 (17)
O8 ⁱ —Ba1—O10	100.97 (17)	O12 ^{iv} —Ba2—O5 ^{vi}	91.34 (16)
O9—Ba1—O9 ⁱⁱ	152.31 (14)	O11—Ba2—O6 ^v	69.21 (18)
O9—Ba1—O10	140.89 (17)	O12—Ba2—O6 ^v	98.07 (17)
O9 ⁱⁱ —Ba1—O10	66.07 (18)	O12 ^{iv} —Ba2—O6 ^v	102.88 (17)
O3—Ba2—O3 ⁱⁱⁱ	157.46 (7)	O11—Ba2—O12	65.67 (18)
O3—Ba2—O4 ⁱⁱⁱ	132.13 (16)	O11—Ba2—O12 ^{iv}	131.22 (17)
O3—Ba2—O5 ^v	72.38 (15)	O12—Ba2—O12 ^{iv}	156.98 (14)
O3—Ba2—O5 ^{vi}	86.55 (16)	Ba1—O9—Ba1 ⁱ	98.34 (17)
O3—Ba2—O6 ^v	108.58 (17)	Ba1—O2—Ba1 ⁱⁱ	100.63 (15)
O3—Ba2—O11	73.36 (16)	Ba1—O8—Ba1 ⁱⁱ	100.27 (15)

Symmetry codes: (i) $-x+1, y-1/2, -z+3/2$; (ii) $-x+1, y+1/2, -z+3/2$; (iii) $-x, y+1/2, -z+3/2$; (iv) $-x, y-1/2, -z+3/2$; (v) $x-1, -y+1/2, z-1/2$; (vi) $-x+1, -y+1, -z+2$.

Table S10. Selected bond lengths (Å) and angles (°) for **4**

Mg1—O1	2.032 (2)	Mg2—O2	2.056 (2)
Mg1—O3	1.996 (2)	Mg2—O4	2.034 (2)
Mg1—O7 ⁱ	2.001 (2)	Mg2—O6	2.054 (2)
Mg1—O5	2.058 (2)	Mg2—O8	2.009 (2)
Mg1—O10	2.036 (2)	Mg2—O9	2.010 (2)
Mg2—O1	2.290 (2)	O1—Mg2—O9	158.92 (8)
O1—Mg1—O5	92.00 (10)	O1—Mg1—O3	99.03 (10)
O1—Mg1—O7 ⁱ	114.10 (10)	O2—Mg2—O4	161.51 (8)
O1—Mg1—O10	94.91 (9)	O2—Mg2—O6	85.51 (10)
O3—Mg1—O5	88.17 (11)	O2—Mg2—O8	92.12 (10)
O3—Mg1—O7 ⁱ	146.87 (9)	O2—Mg2—O9	99.13 (9)
O3—Mg1—O10	88.58 (8)	O4—Mg2—O6	90.91 (9)
O5—Mg1—O7 ⁱ	90.68 (10)	O4—Mg2—O8	90.29 (9)
O5—Mg1—O10	172.75 (8)	O4—Mg2—O9	99.03 (9)
O7 ⁱ —Mg1—O10	88.50 (10)	O6—Mg2—O8	175.92 (8)
O1—Mg2—O2	59.95 (8)	O6—Mg2—O9	90.28 (9)
O1—Mg2—O4	101.73 (8)	O8—Mg2—O9	93.38 (9)
O1—Mg2—O6	85.78 (10)	Mg1—O1—Mg2	107.80 (9)
O1—Mg2—O8	90.15 (10)		

Symmetry codes: (i) $x, -y+3/2, z-1/2$; (ii) $-x+1, -y+2, -z+1$; (iii) $-x+2, y-1/2, -z+1/2$; (iv) $-x+1, -y+1, -z+1$; (v) $x, -y+3/2, z+1/2$; (vi) $-x+2, y+1/2, -z+1/2$.

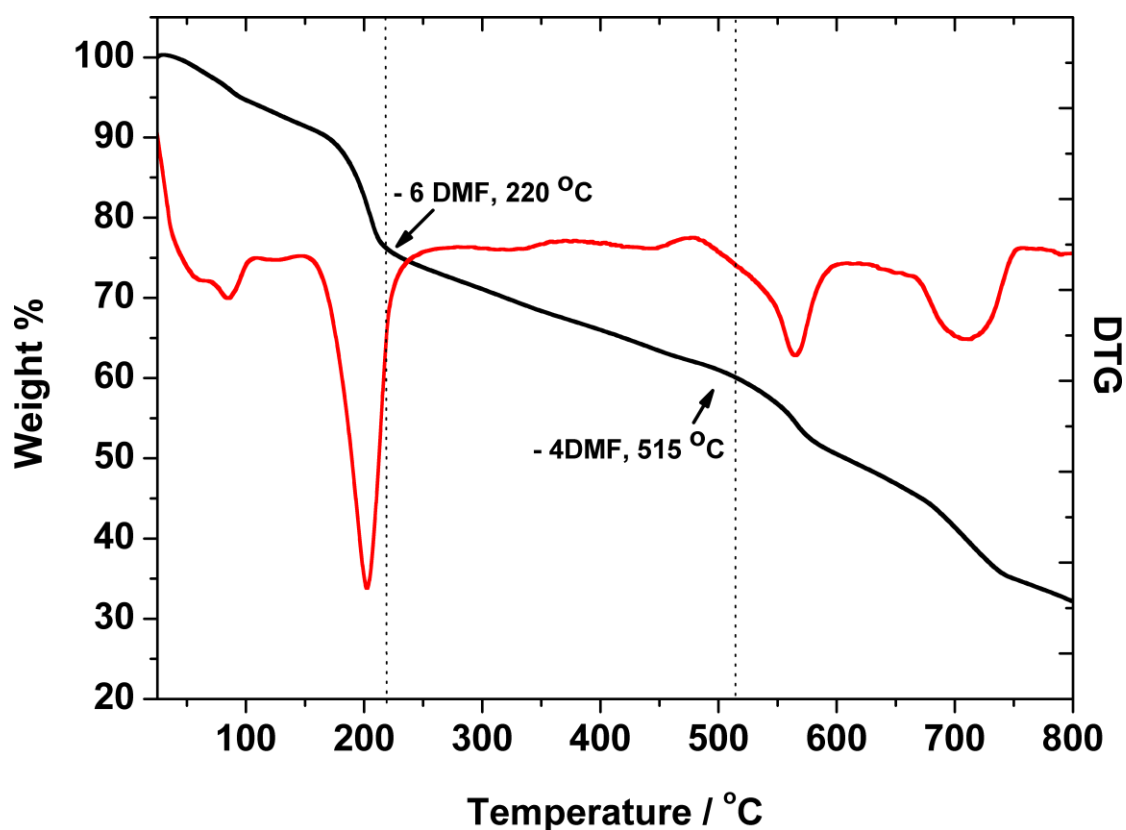


Figure S20. The TG (black line) and DTG (first derivative) curves for **1**.

The TGA data indicate the weight losses starting from 60 °C and ending at over 800 °C. In the first two steps (60-220 °C) we observed weight loss which corresponds to the removal of six guest DMF molecules located inside the pores of the MOF experimental loss of 22.89 %, theoretically estimated loss of 23.99 %). The following weight loss (220-515 °C) is due to the release of the coordinated DMF molecules experimental loss of 15.76 %, theoretically estimated loss of 15.99 %), the before decomposition of the framework sets in.

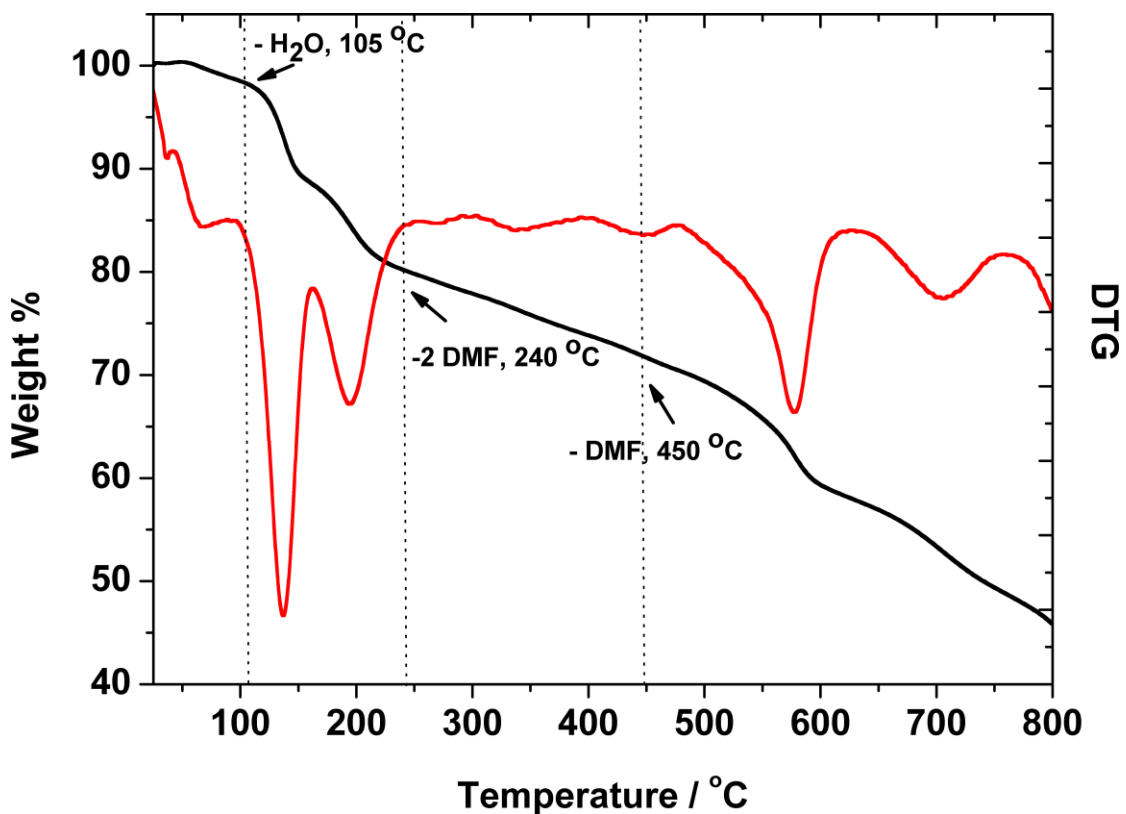


Figure S21. The TG (black line) and DTG (first derivative) curves for **2**.

The TGA data indicate the weight losses starting from 70 °C and ending at over 800 °C. The weight loss was observed in four steps. In the first step (50-105 °C) we observe weight loss of the coordinated water molecules (experimental loss of 2.09 %, theoretically estimated loss of 2.07 %). The following stages (105-450 °C) can be attributed to the release of the guest and terminal DMF molecules (experimental loss of 26.59 %, theoretically estimated loss of 25.20 %), followed by the decomposition of the framework.

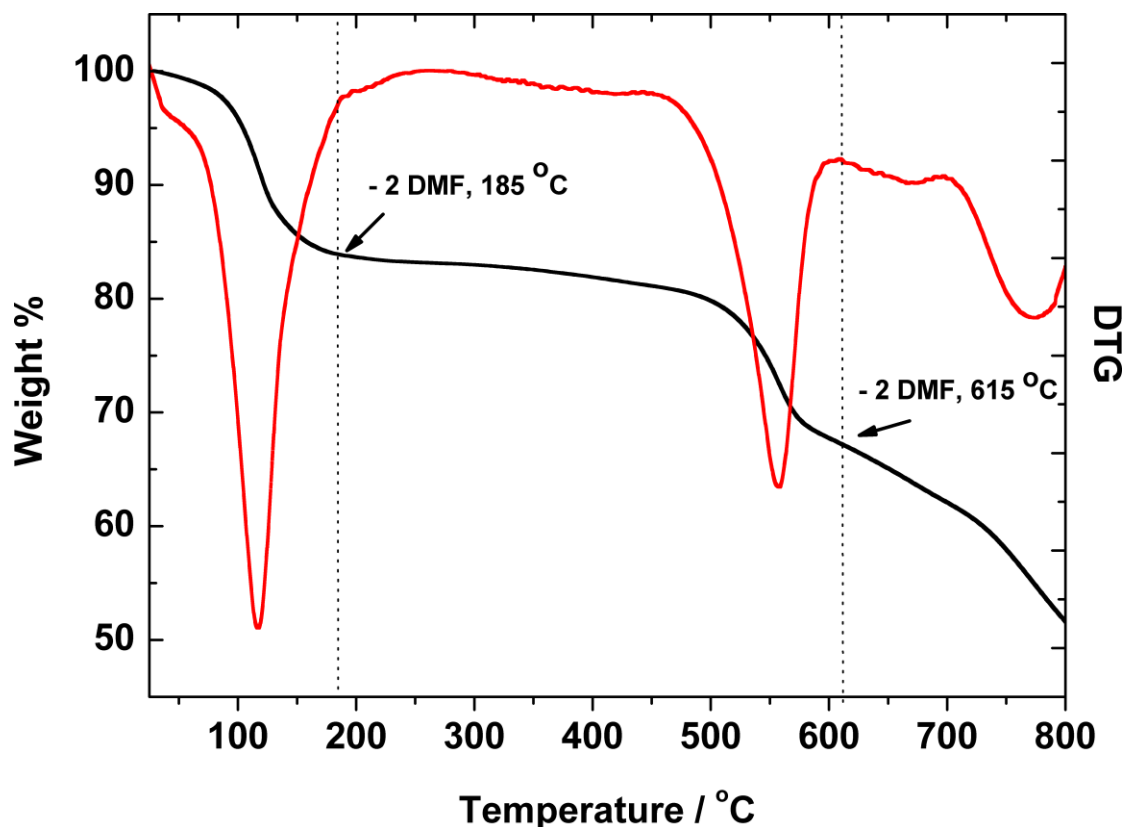


Figure S22. The TG (black line) and DTG (first derivative) curves for **3**.

The TGA data indicate the weight losses starting from 70 °C and ending at over 800 °C. The weight loss was observed in three steps. The first weight loss occurring from 70 °C to 185 °C corresponds to the loss of the coordinated DMF molecules (experimental loss of 14.79%, theoretically estimated loss of 14.25%). The thermal intermediate remains stable up to 460 °C where the second weight loss begins, which is completed at 605 °C. This stage corresponds to the loss of the bridging DMF molecules (experimental loss of 13.66%, theoretically estimated loss of 14.25%). The last stage involves the decomposition of the organic ligand which leads to the collapse of the framework.

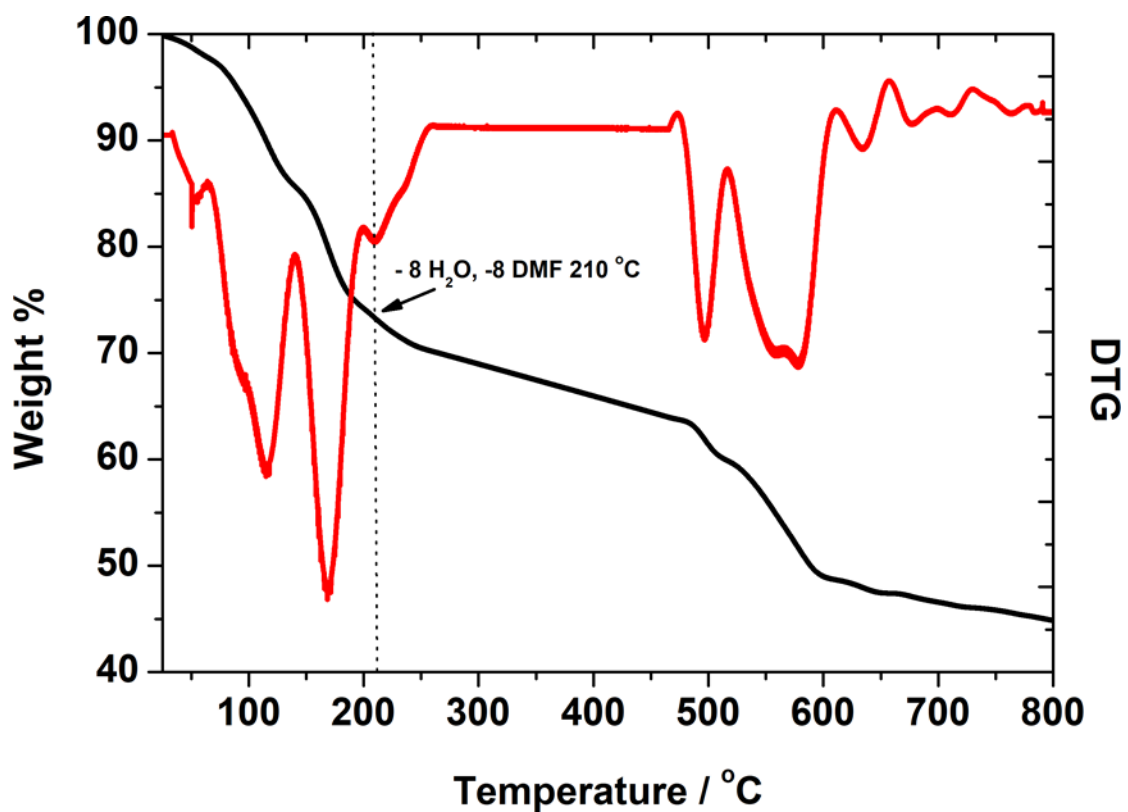


Figure S23. The TG (black line) and DTG (first derivative) curves for **4**.

The weight loss of **4** was observed in two discrete steps. The first weight loss (65-210 °C) can be possibly assigned to the loss of the coordinated and guest water and DMF molecules (experimental loss of 24.55 %, theoretically estimated loss of 24.54 %) before the decomposition of the framework sets in.

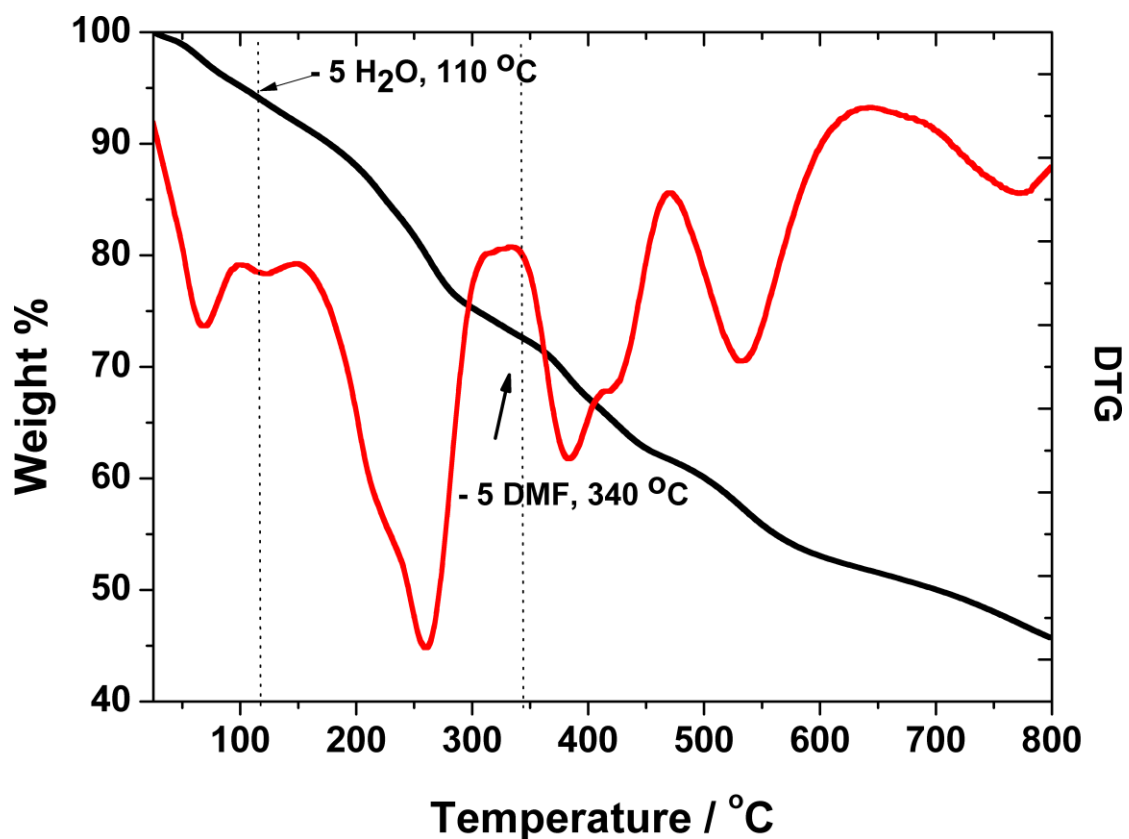


Figure S24. The TG (black line) and DTG (first derivative) curves for **5**.

The TGA data indicate continuous weight losses starting from 25 °C and ending at over 800 °C. The weight losses occurring from 25-110 °C are attributed to the removal of five water molecules (experimental loss of 5.54 %, theoretically estimated loss of 5.59 %). The following weight losses occurring from 110 to 340 °C are assigned to the release of the coordinated and guest DMF molecules. The last weight loss is attributed to the decomposition of the organic ligands.

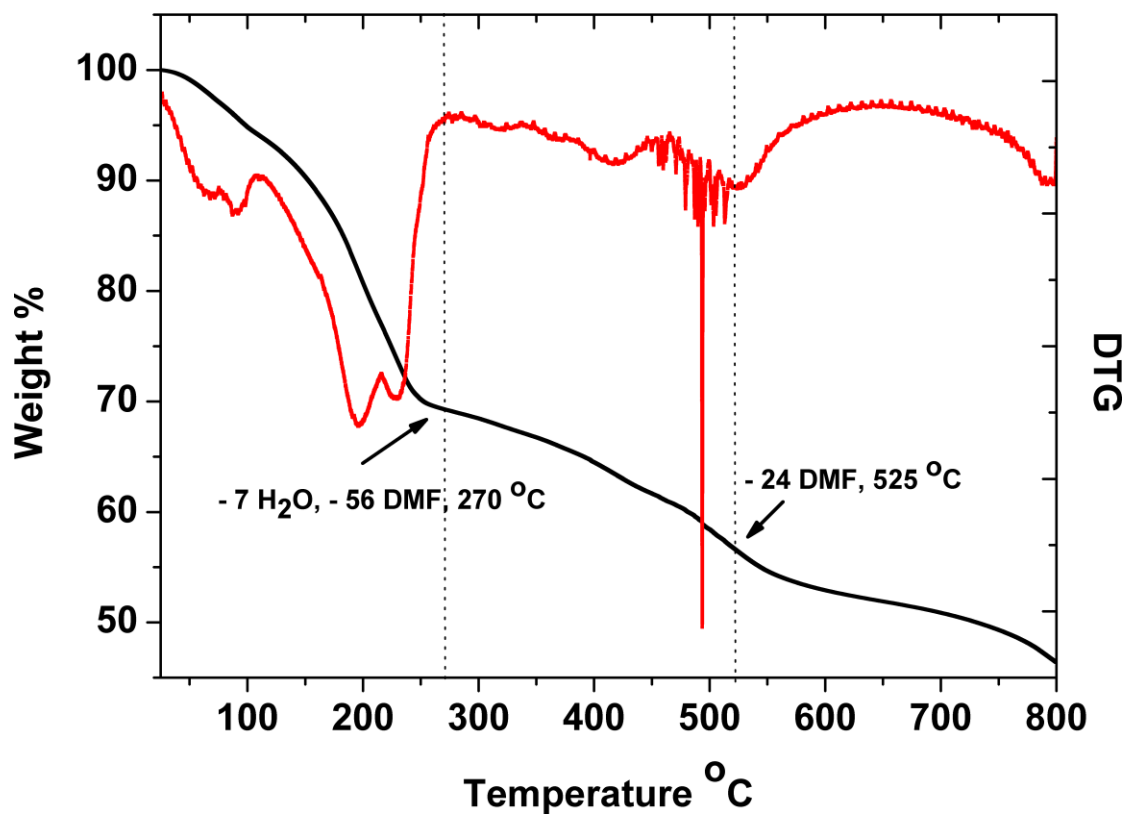


Figure S25. The TG (black line) and DTG (first derivative) curves for **6**.

The weight loss of **6** was observed in three steps. The first weight loss (25-270 °C) corresponds to the release of the guest DMF and water molecules (experimental loss of 30.90 %, theoretically estimated loss of 30.77 %). The second step (270-525 °C) involves the loss of the coordinated DMF molecules (experimental loss of 12.79 %, theoretically estimated loss of 12.81%), which leads to the collapse of the framework.

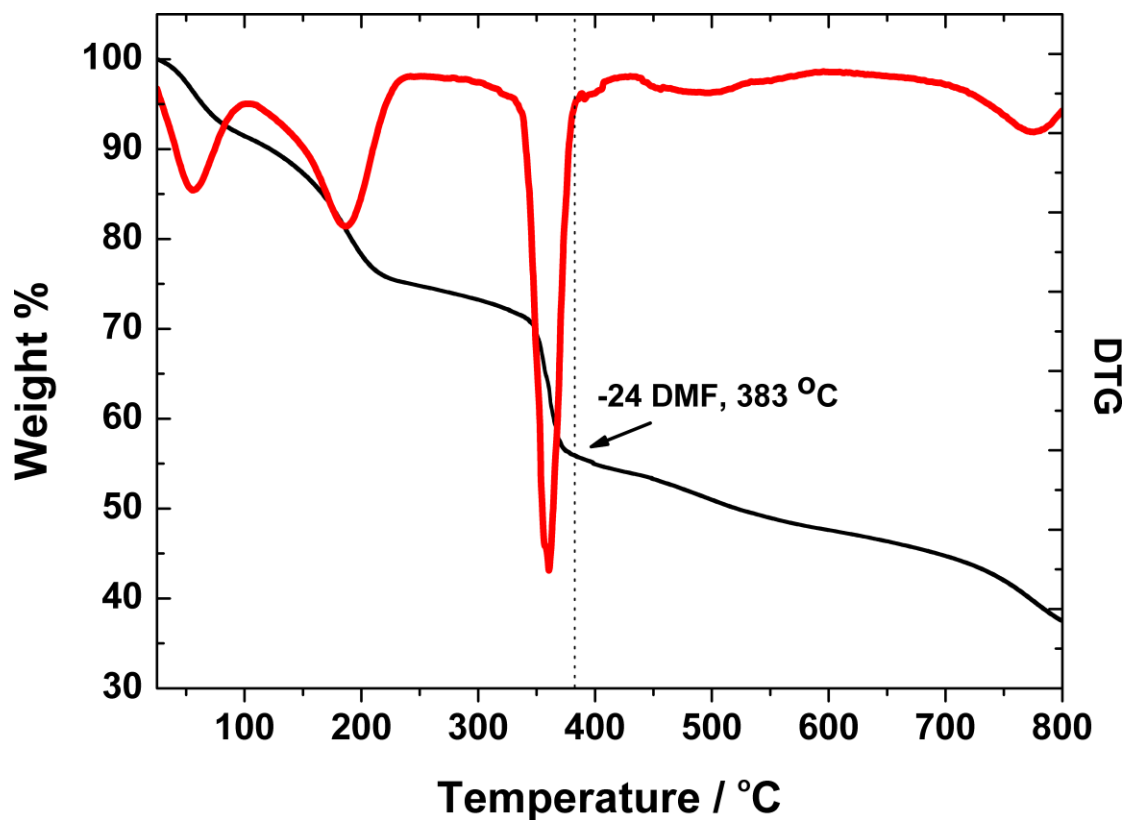


Figure. S26. The TG (black line) and DTG (first derivative) curves for **7**.

The weight loss of **7** was observed in two discrete steps. The first weight loss (100-383 °C) corresponds to the removal of twenty four coordinated and guest DMF molecules (experimental loss of 35.89%, theoretically estimated loss of 35.91%) before decomposition of the framework sets in

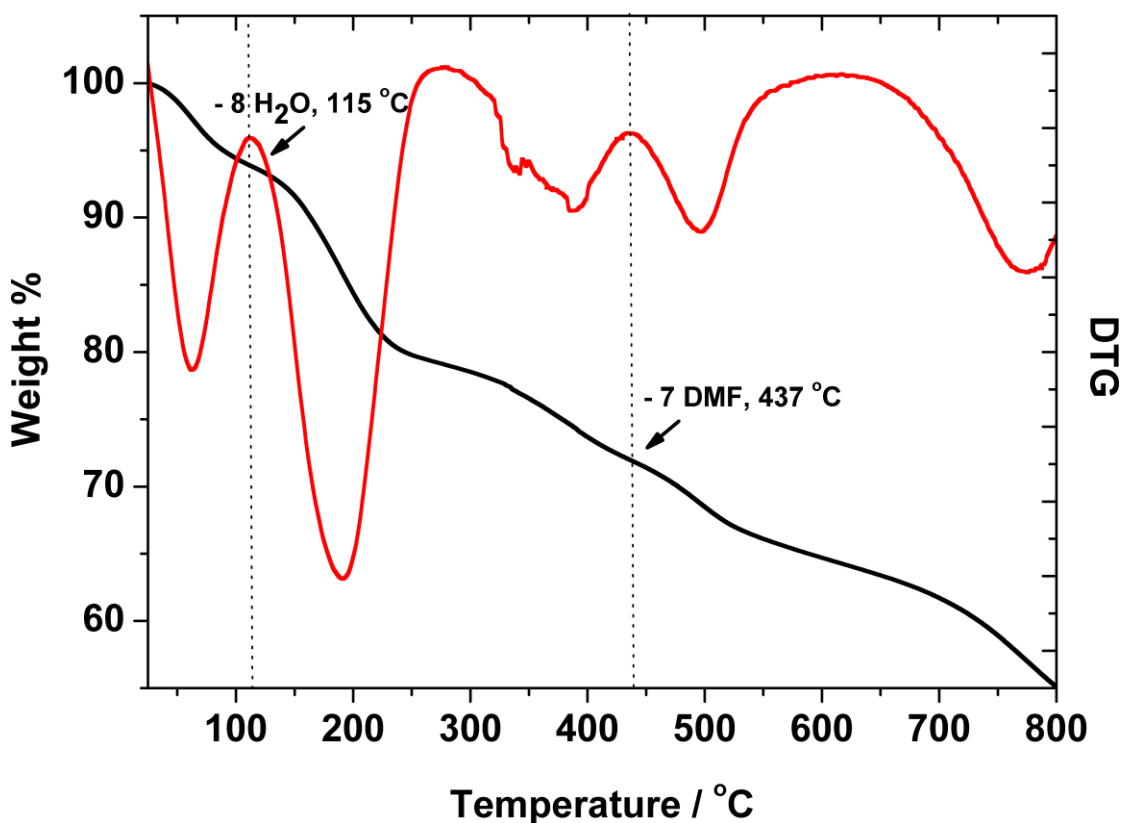


Figure S27. The TG (black line) and DTG (first derivative) curves for **8**.

The TGA data indicate the weight losses starting from 40 °C and ending at over 800 °C. In the first two steps (40-115 °C), we observed weight loss which corresponds to the removal of eight coordinated water molecules (experimental loss of 5.78 %, theoretically estimated loss of 6.15 %). The following weight loss (115-473 °C) is likely due to the release of the guest DMF molecules (experimental loss of 21.99 %, theoretically estimated loss of 21.86 %), and it leads to the collapse of the framework.

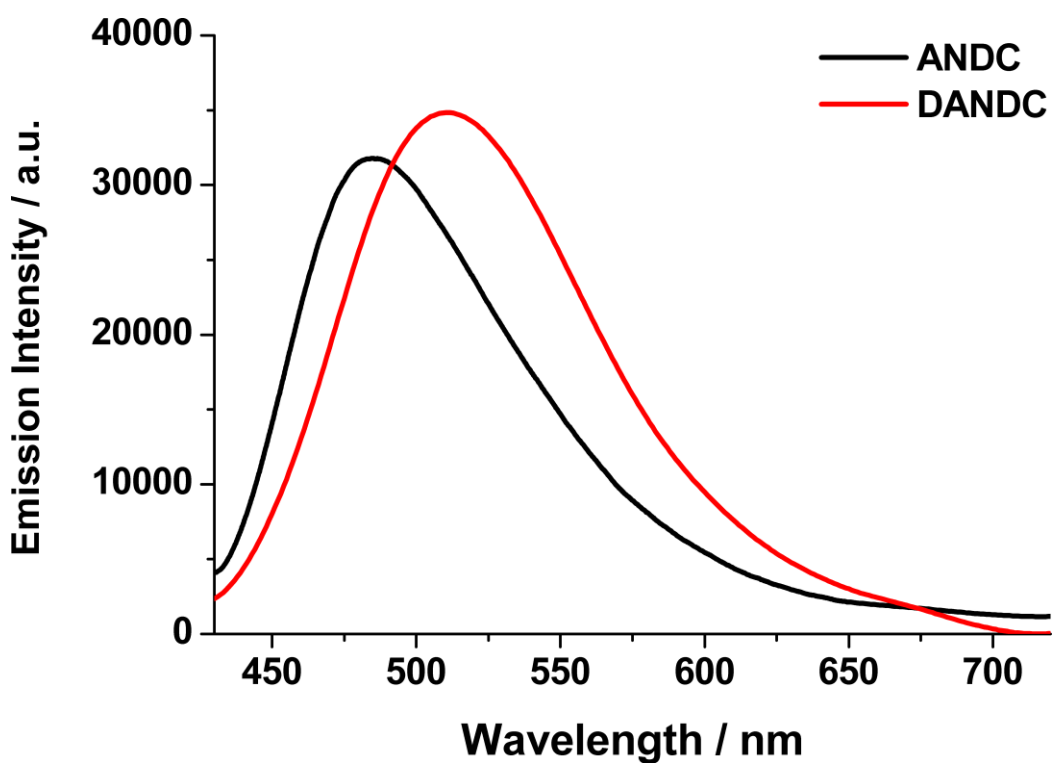


Figure S28. Emission spectra of the ligands in MeOH upon excitation at ligand's maximum absorption (370 nm and 400 nm respectively).

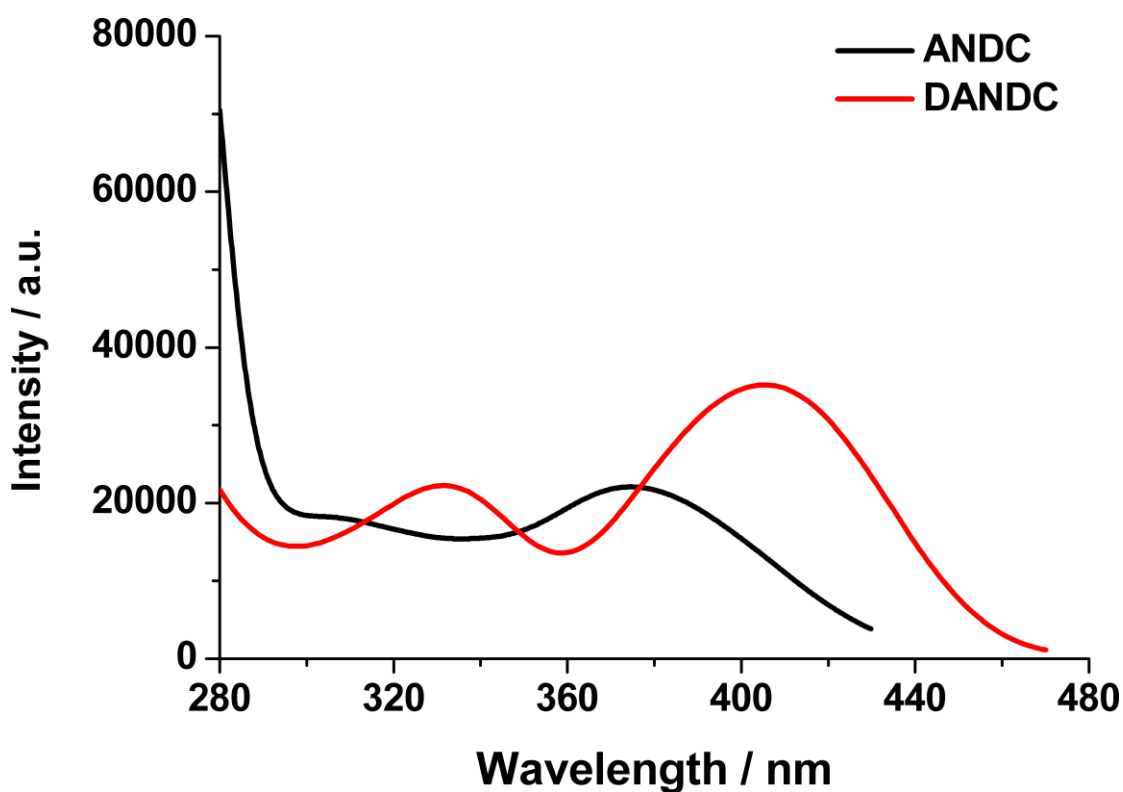


Figure S29. Excitation spectra of the ligands in MeOH upon excitation at ligand's maximum absorption ($\lambda_{\text{mon}} =$ nm and 400 nm respectively).

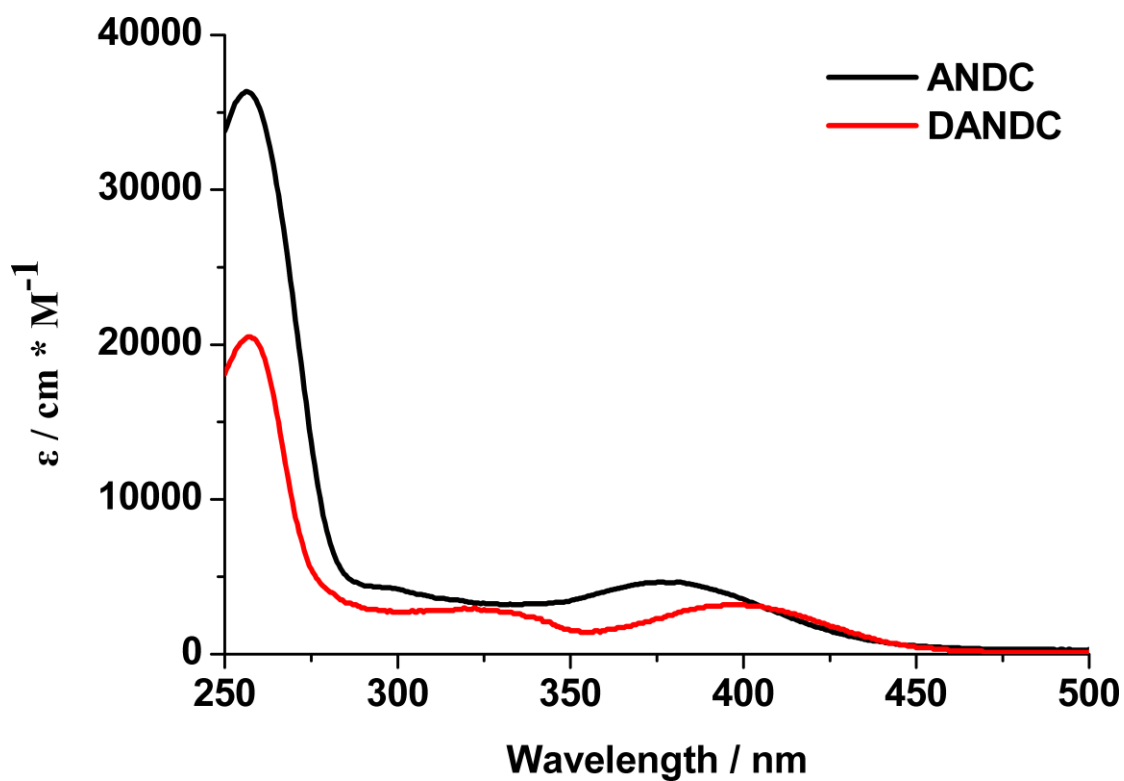


Figure S30. UV-Vis spectra of the ligands in MeOH solution.

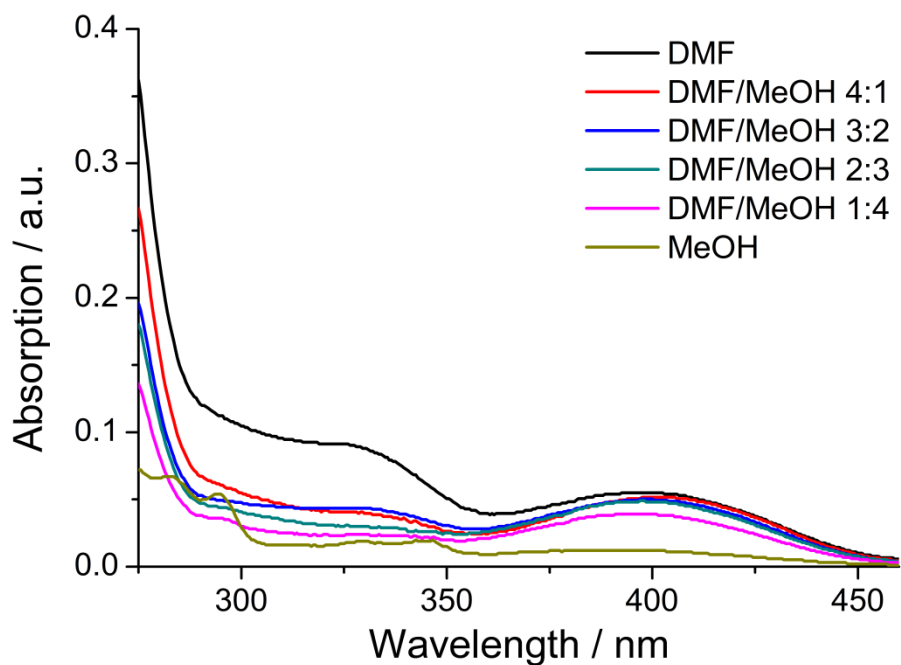


Figure S31. UV-Vis spectra of the H₂ANDC ligand in DMF/MeOH mixtures.

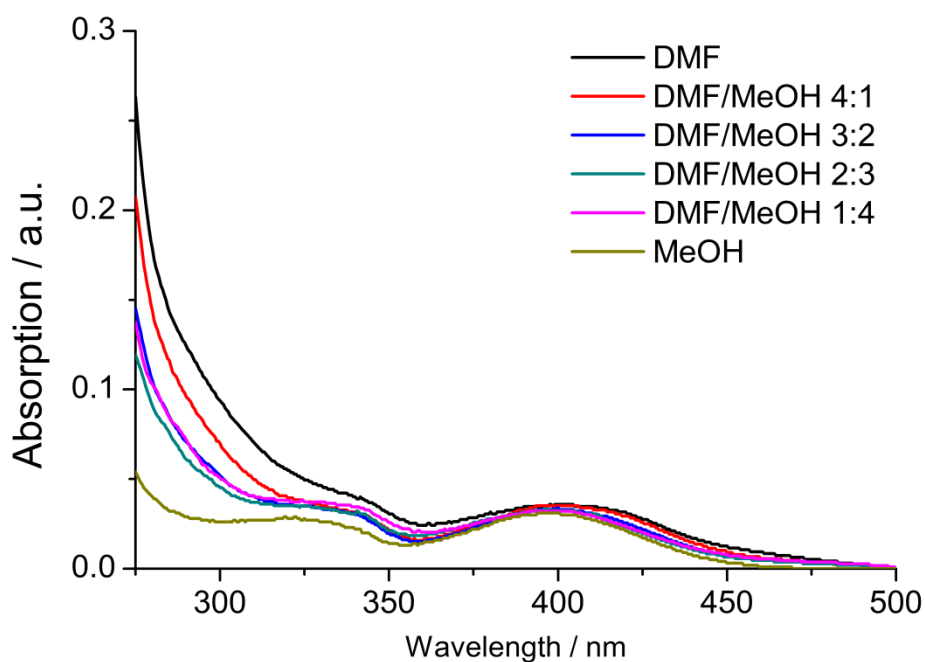


Figure S32. UV-Vis spectra of the H₂DANDC ligand in DMF/MeOH mixtures.

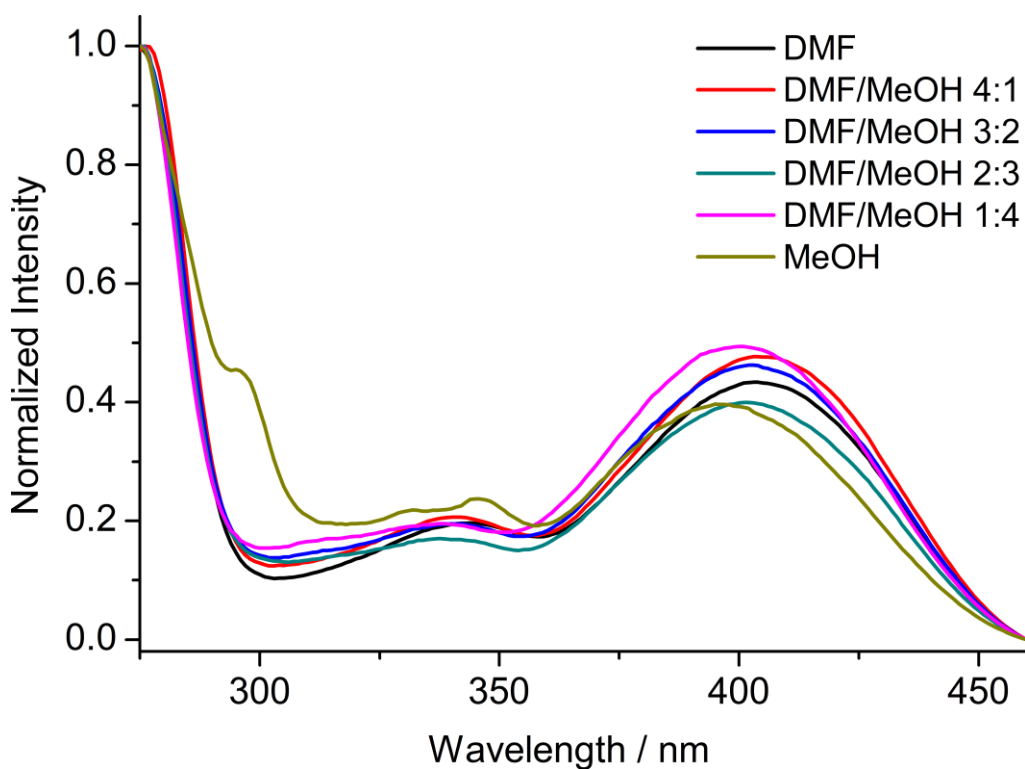


Figure S33. Excitation spectra of the H₂ANDC ligand in DMF/MeOH mixtures monitored at the emission maxima.

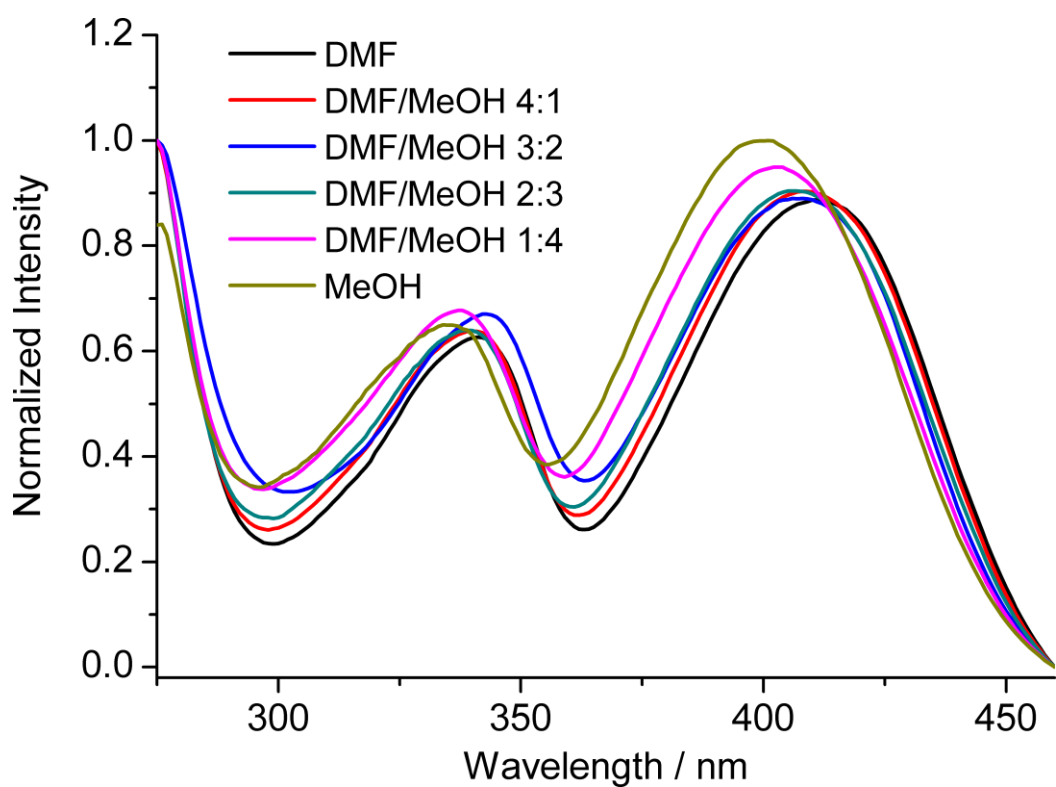


Figure S34. Excitation spectra of the H₂DANDC ligand in DMF/MeOH mixtures monitored at the emission maxima.

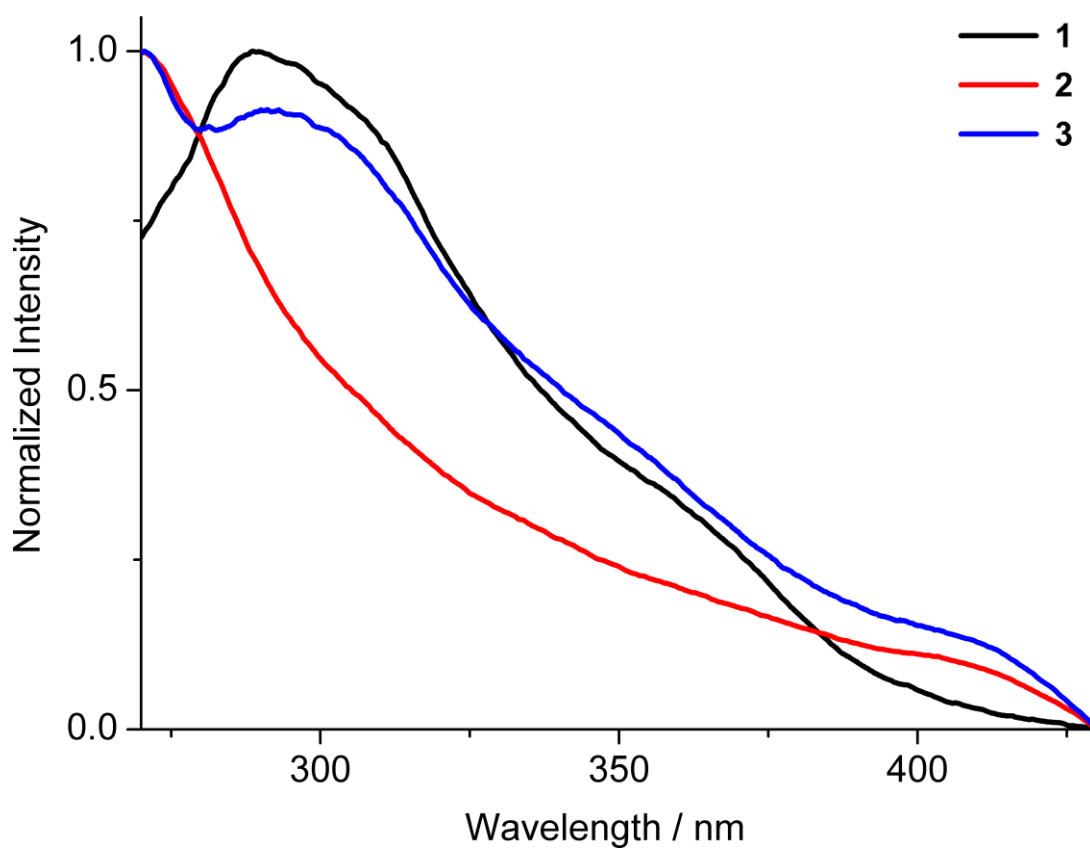


Figure S35. Excitation spectra of **1-3** monitored at the emission maxima.

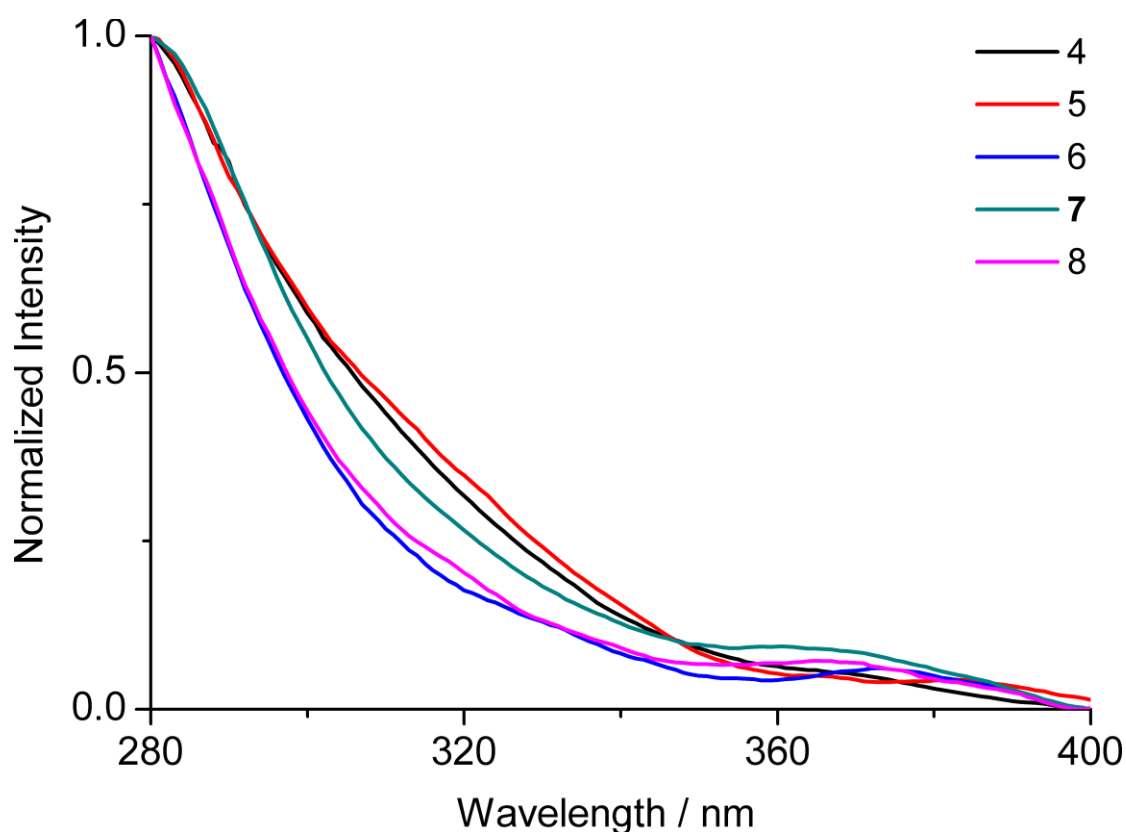


Figure S36. Excitation spectra of **4-8** monitored at the emission maxima.

References

1. S. A. Diamantis, A. D. Pournara, A. G. Hatzidimitriou, M. J. Manos, G. S. Papaefstathiou and T. Lazarides, *Polyhedron*, 2018, **153**, 173-180.
2. J. Sim, H. Yim, N. Ko, S. B. Choi, Y. Oh, H. J. Park, S. Park and J. Kim, *Dalton Transactions*, 2014, **43**, 18017-18024.
3. I. A. Bruker, *Analytical X-ray Systems*, Madison, WI, 2006.
4. I.S.A.-D.A.C.M, *Siemens Industrial Automation*, 1996.
5. P. W. Betteridge, J. R. Carruthers, R. I. Cooper, K. Prout and D. J. Watkin, *Journal of Applied Crystallography*, 2003, **36**, 1487.
6. L. Palatinus and G. Chapuis, *Journal of Applied Crystallography*, 2007, **40**, 786-790.
7. C. F. Macrae, P. R. Edgington, P. McCabe, E. Pidcock, G. P. Shields, R. Taylor, M. Towler and J. van de Streek, *Journal of Applied Crystallography*, 2006, **39**, 453-457.